Testing the ability of in-vitro depletion rates to assess the biotransformation rate and bioconcentration factor of hydrophobic chemicals in rainbow trout (*Oncorhynchus mykiss*)

by
Kapilan Ratneswaran

B.Sc. (Hon. Biology), Wilfrid Laurier University, 2015

Project Submitted in Partial Fulfillment of the

Requirements for the Degree of

Master of Environmental Toxicology

in the

Department of Biological Sciences

Faculty of Science

SIMON FRASER UNIVERSITY

Fall 2018

Approval

Name:	**Kapilan Ratneswaran**
Degree:	**Master of Environmental Toxicology**
Title:	**Testing the ability of in-vitro depletion rates to assess the biotransformation rate and bioconcentration factor of hydrophobic chemicals in rainbow trout (*Oncorhynchus mykiss*)**
Examining Committee:	**Chair:** Felix Breden Professor

Frank Gobas
Senior Supervisor
Professor

Christopher Kennedy
Supervisor
Professor

Vicki Marlatt
Examiner
Assistant Professor

Date Defended/Approved: December 3, 3018

Ethics Statement

The author, whose name appears on the title page of this work, has obtained, for the research described in this work, either:

a. human research ethics approval from the Simon Fraser University Office of Research Ethics

or

b. advance approval of the animal care protocol from the University Animal Care Committee of Simon Fraser University

or has conducted the research

c. as a co-investigator, collaborator, or research assistant in a research project approved in advance.

A copy of the approval letter has been filed with the Theses Office of the University Library at the time of submission of this thesis or project.

The original application for approval and letter of approval are filed with the relevant offices. Inquiries may be directed to those authorities.

Simon Fraser University Library
Burnaby, British Columbia, Canada

Update Spring 2016

Abstract

The objective of this study was to test the ability of in-vitro biotransformation rates to predict in-vivo biotransformation rates and BCFs to ultimately improve chemical bioaccumulation assessment. In-vitro biotransformation rates of hydrophobic chemicals pyrene, methoxychlor, cyclohexyl salicylate, and 2,6 dimethyldecane were determined using a rainbow trout liver S9 preparation and then input into two in-vitro-in-vivo extrapolation (IVIVE) models to estimate in-vivo biotransformation rates (k_{MET}) and modelled BCFs. Comparisons of in-vitro derived k_{MET} values using both IVIVE models were in reasonable agreement when compared to in-vivo derived k_{MET} values for pyrene and methoxychlor. Estimated BCFs from this study for pyrene, methoxychlor, and cyclohexyl salicylate were also in good agreement with estimated BCFs from previous studies using in-vitro biotransformation rates as inputs to IVIVE models, but were significantly higher compared to empirical BCFs. This indicates the potential usefulness of in-vitro biotransformation assays and IVIVE models for estimating k_{MET} and BCFs, however k_{MET} values from IVIVE models and BCF estimates should only be considered a conservative estimate at this time due to the uncertainty (i.e. extrahepatic metabolism) associated with these models and the further work required to fine-tune these models.

Keywords: bioaccumulation; biotransformation; in-vitro-in-vivo extrapolation; rainbow trout liver S9; bioconcentration factor; hydrophobic chemicals

Acknowledgements

There are many people who I would like to acknowledge for their assistance with this MET project. I would like to thank my senior supervisor Dr. Frank Gobas for providing me with the opportunity to work under him as a graduate student. His guidance, support and words of encouragement have allowed me to successfully complete this project, while also developing strong scientific research skills in the field of bioaccumulation science. I would also like to thank Dr. Christopher Kennedy for his guidance and feedback throughout this research project as well. I also express my thanks to Dr. Vicki Marlatt for kindly agreeing to be on my committee as my examiner, and Dr. Felix Breden for chairing my defence.

I am also very grateful to my ToxLab colleagues as well. I would like to thank Victoria Otton for her support since joining the lab, and also for providing really insightful feedback and critical review throughout this project. I am also thankful to Gaya Allard and Leslie Saunders for sharing knowledge of experimental techniques and providing assistance when required. I also thank all the members of Fugacity Club for providing a supportive environment to discuss ideas and for their support.

I am thankful to Alex Fraser and David Qu for their assistance in using equipment from the Biology Department. I thank Bruce Leighton as well for providing me with fish for this experiment. I am also appreciative of the help from members of the Kennedy Lab regarding scientific equipment. I would like to thank Christina Johnston as well for her assistance in perfusing rainbow trout livers for this research. I also appreciate the support of the administrative staffs in the Resource and Environmental Management and Biological Sciences departments throughout this entire process.

Finally, I would like to express my thanks to my parents, my brothers, my sister in law, and my aunts and uncles for their constant words of encouragement and support throughout these years.

Table of Contents

List of Tables

List of Figures

List of Acronyms

ANOVA	Analysis of variance
B	Bioaccumulative
BAF	Bioaccumulation Factor
BCF	Bioconcentration Factor
BSA	Bovine Serum Albumin
$C_{ACTIVE\ S9}$	Concentration of test chemical in active S9
$C_{INACTIVE\ S9}$	Concentration of test chemical in inactive S9
CEPA	Canadian Environmental Protection Act
CL_H	Hepatic clearance rate
$CL_{IN\ VITRO,INT}$	In-vitro intrinsic clearance
$CL_{IN\ VIVO,INT}$	In-vivo intrinsic clearance
CV	Coefficient of Variation
CYP	Cytochrome P450
DSL	Domestic Substances List
EU	European Union
EVA	Ethylene Vinyl Acetate
f_U	Hepatic clearance binding term
GC/MS	Gas Chromatography-Mass Spectrometry
GST	Glutathione S-transferases
I.S.	Internal Standard
IVIVE	In-vitro-in-vivo extrapolation
k_2	Catalytic step
k_{dep}	In-vitro depletion rate constant
K_M	Michaelis constant
k_{MET}	Whole organism biotransformation rate constant
$k_{MET,H}$	In vivo hepatic biotransformation rate constant
$k_{MET,10g}$	Whole organism biotransformation rate constant normalized to 10 g fish
K_{OW}	Octanol Water Partition Coefficient
Ln	Natural logarithm
m/z	Mass-charge ratio
MS-222	Tricaine methanesulfonate

NAT	N-acetyltransferases
OECD	Organisation for Economic Co-operation and Development
OECD TG	Organisation for Economic Co-operation and Development Test Guideline
P	Persistent
PAH	Polycyclic Aromatic Hydrocarbon
PBT	Persistence, Bioaccumulation, Toxicity
PCB	Polychlorinated Biphenyl
PCR	Polymerase Chain Reaction
REACH	Registration, Evaluation, Authorisation and Restriction of Chemicals
S9	Supernatant fraction from liver homogenate after centrifuging at 9000 g
SEM	Standard Error of the Mean
SD	Standard Deviation
SF	Scaling Factor
SFU	Simon Fraser University
SPME	Solid phase microextraction
SULT	Sulfotransferases
T	Inherently Toxic
TSCA	Toxic Substances Control Act
TRI	Toxic Release Inventory
Tukey's HSD	Tukey's Honestly Significant Difference Test
UGT	UDP-glucuronosyltransferases
V_{MAX}	Theoretical maximum of metabolic rate

Introduction

The continued production, use and release of anthropogenic chemicals and their potential to cause harm to humans and the environment is a major concern. In particular, chemicals that have the ability to persist (P) in the environment for long periods of time, bioaccumulate (B) in organisms and food webs, and are considered to be toxic (T) are especially a concern. A global effort is currently underway to evaluate their potential for persistence, bioaccumulation and toxicity (PBT) to ensure that they are properly regulated and that the risks associated with them are well understood and mitigated. However, the number of chemicals to be evaluated is large. For example, more than 140,000 man-made chemicals were estimated to be on the European market in and the total volume of chemicals produced rose by 54% between 2000 to 2010 (UNEP, 2013).

1.1 Current regulation of chemicals

Various regulatory agencies across the world are responsible for assessing chemical risks within their own jurisdictions. For instance the Registration, Evaluation, Authorisation and Restriction of Chemicals (REACH) is the set of regulations used to assess the risks of chemicals within the European Union (E.U.). In Canada, Health Canada and Environment and Climate Change Canada adhere to a set of regulations outlined in the Canadian Environmental Protection Act (CEPA). Although the specific regulatory criteria for the assessment of persistence (P), bioaccumulation (B), and toxicity (T) vary between jurisdictions, all of these regulatory agencies include the assessment of chemicals for persistence (P), bioaccumulation (B), and toxicity (T).

In Canada, the Domestic Substances List (DSL), first published in 1994 by Environment Canada, lists approximately 23,000 substances that were imported or manufactured in Canada between January 1984 and December 1986 (existing substances). Per CEPA guidelines, substances on the DSL were categorized. By comparing persistence, bioaccumulation, and toxicity information of chemicals to established criteria, if the chemicals meet the criteria for PBT then the substances are further evaluated for their potential toxicity. Substances not on the list have to be reported prior to being put in commerce and assessed for their toxic potential to human health and the environment. As mentioned earlier, Health Canada and Environment and

Climate Change Canada are the regulatory agencies responsible for this assessment. The specific criteria that Environment and Climate Change Canada is using are described in Table 1.1. The evaluation of the persistence (P) of chemicals assesses the duration that chemicals remain in the environment before being degraded, and relies on comparing half-life values of chemicals (the amount of time it takes a chemicals to degrade in the environment by 50%) to established CEPA criteria (Environment and Climate Change Canada 2013). Toxicity (T) evaluation of chemicals assesses the potential for chemicals to harm the environment and human health by comparing toxicity data for mammals and aquatic organisms (i.e. LC50 and LD50 values) to established criteria (Environment and Climate Change Canada 2013). Lastly, bioaccumulation (B) evaluation is based on determining and comparing bioaccumulation factors (BAFs), bioconcentration factors (BCFs), and the octanol water partition coefficient (K_{OW}) to established criteria (Environment and Climate Change Canada 2013). Taken together, if a chemical exceeds the established values related to any of these three criteria, a more comprehensive assessment of the chemical is completed to assess the potential risks of the chemical.

Table 1.1. CEPA Persistence (P), bioaccumulation (B), and toxicity (T) criteria for assessing substances on the DSL.

Persistence (P)		**Bioaccumulation (B)**	**Toxicity (T)**
Environmental Media	**Half Life ($t_{1/2}$)**		
Water	≥ 180 days	BCF ≥ 5000	
Air	≥ 2 days	BAF ≥ 5000	CEPA toxic
Soil	≥ 180 days	Log K_{OW} ≥ 5	
Sediment	≥ 365 days		

However, a major issue with screening chemicals based on these criteria is the lack of available data. This is particularly true for the bioaccumulation assessment, as it has been reported that only 4% of chemicals listed on the Canadian Domestic Substances List (DSL) have actual empirical data related to bioaccumulation endpoints when compared to toxicity and persistence endpoints (Weisbrod et al. 2009; Arnot and Gobas 2006). Thus, a need existed for improving the accuracy of bioaccumulation assessment as well as expanding the resources required to gather relevant data on bioaccumulation endpoints (Weisbrod et al. 2009).

1.2 Current bioaccumulation criteria

Currently, bioaccumulation screening criteria is based on three endpoints: bioconcentration factors (BCFs), bioaccumulation factors (BAFs), and the octanol-water partition coefficient (K_{OW}). The BCF is the ratio of the concentration of a substance in an organism to the concentration in water, and is based on uptake of the chemical from the surrounding water. The BAF is also a measurement of the ratio of the concentration of a substance in an organism to the concentration in water, but takes into account chemical uptake from surrounding water and from food. The K_{OW} is a measure of the ratio of the chemical concentration in octanol and water in an octanol-water system at equilibrium. The K_{OW} is a measure of the hydrophobicity of a chemical and it also is used to describe how a chemical would partition between the lipids in an organism and the surrounding water (Arnot and Gobas 2006). BCF measurements can be obtained only within a lab setting, while BAF measurements are typically obtained in the field.

Table 1.2. Overview of current bioaccumulation assessment endpoints and criteria across various regulatory agencies (Adapted from Arnot and Gobas 2006).

Regulatory Agency	Bioaccumulation Endpoint	Criteria	Program
Environment Canada	BAF	≥ 5000	CEPA*
Environment Canada	BCF	≥ 5000	CEPA
Environment Canada	log Kow	≥ 5.0	CEPA
European Union "Bioaccumulative"	BCF	≥ 2000	REACH†
European Union "Very Bioaccumulative"	BCF	≥ 5000	REACH
United States "Bioaccumulative"	BCF	1000-5000	TSCA, TRI‡
United States "Very Bioaccumulative"	BCF	≥ 5000	TSCA, TRI
United Nations Environment Programme	BCF	≥ 5000	Stockholm Convention€
United Nations	log K_{OW}	≥ 5.0	Stockholm

Environment Programme			Convention

* CEPA, Canadian Environmental Protection Act, 1999 (Government of Canada, 1999; Government of Canada 2000)
† Registration, Evaluation and Authorization of Chemicals (REACH) Annex XII (European Commission 2001)
‡ Currently being used by the US Environmental Protection Agency in its Toxic Substance Control Act (TSCA) and Toxic Release Inventory (TRI) programs (USEPA 1976)
€ Stockholm Convention on Persistent Organic Pollutants (UNEP 2001)

Despite the use of these endpoints in the screening process for bioaccumulation, there are limitations associated with them. A potential drawback to BCF values is that it could potentially underestimate bioaccumulation potential of a chemical if dietary uptake is a major route of exposure (Nichols et al. 2007). BAF values, while being the most environmentally relevant endpoints, are very expensive to measure and the potential for site-specific factors to influence BAF measurements remains a potential area of concern (Nichols et al., 2007). The major limitation of BCF and BAF criteria is that they are unavailable for most chemicals (Arnot and Gobas 2006). Bioconcentration testing can be performed (ie. OECD 305) to assess bioaccumulation potential of substances, but these tests are expensive to complete, time-consuming and require a large number of animals (Weisbrod et al. 2009). For example, it has been reported that the OECD 305 in-vivo bioconcentration test takes 3-6 months to complete and costs an average of $125 000 per chemical (Weisbrod et al. 2009).

Thus, K_{OW} and K_{OW}-based accumulation models are heavily relied upon to conduct bioaccumulation screening. KOW values are easy and inexpensive to measure, or they can be predicted using specific software (e.g., EPI Suite). However the use of K_{ow} in bioaccumulation assessment may be inadequate as it does not include any physiological processes such as active uptake/loss of chemicals via gills or biotransformation (Dyer et al. 2008). The exclusion of biotransformation in K_{ow} is a major limitation, as the potential exists for chemicals to be screened as bioaccumulative using K_{ow} values when they are not (ie. false positive). This is because chemicals may be biotransformed via enzymatic conversion of hydrophobic parent compounds to more readily excretable metabolites, thus attenuating their bioaccumulation. Many studies have demonstrated the importance of biotransformation in BCF determination in fish (Han et al. 2007; Laue et al. 2014; Han et al. 2009; Cowan-Ellsberry et al. 2008). BCF values which were estimated with consideration of biotransformation were closer to the BCF values measured in vivo, compared to the BCF predictions made without biotransformation data. Thus, through the use of in-vitro assays involving fish hepatocytes, liver microsomes, and

S9 fractions followed by the extrapolation of in-vitro biotransformation rates to the in-vivo level, in-vitro testing has the potential to be useful in predicting the bioaccumulation potential of chemicals.

1.2.1 In-vitro biotransformation rate studies

In-vitro testing strategies have been proposed as one method to investigate biotransformation and to assess the bioaccumulation potential of chemicals and to reduce animal testing for bioaccumulation assessments. The benefits of *in-vitro* tests over *in-vivo* testing include: a reduction in cost, the use of significantly fewer animals, a reduction in time required to conduct the tests, and potentially, the ability to test several chemicals simultaneously (Nichols et al. 2007). The inclusion of hepatic biotransformation rates obtained from in-vitro assays into an in-vitro to in-vivo extrapolation model (IVIVE) is widely used in the pharmaceutical industry to predict the contribution of biotransformation in the overall elimination of drugs (Rane et al. 1977; Obach 1999). This IVIVE method has been adopted for the assessment of bioconcentration factors in fish (Nichols et al. 2006; Nichols et al. 2013a).

Briefly, IVIVE involves using the biotransformation rate measured in *in-vitro* assays to determine the *in-vitro* intrinsic clearance ($CL_{IN\ VITRO,INT}$; mL/h/mg protein) of the test chemical, followed by estimation of *in-vivo* intrinsic clearance ($CL_{IN\ VIVO,INT}$; mL/h/g fish). The hepatic clearance rate (CL_H) is then determined based on the well stirred liver model of Wilkinson and Shand (1975) (Nichols et al. 2013a). Finally, the *in-vivo* biotransformation rate (k_{MET}) is determined and then input into a fish bioaccumulation model to predict the BCF value (Arnot and Gobas 2004).

In-vitro assays involving hepatic drug biotransformation are often conducted using different liver preparations: S9 subcellular fractions, freshly prepared hepatocytes, cryopreserved hepatocytes and microsomes. The choice of in-vitro assay system is often based on the specific study in question, monetary costs, as well as what metabolic enzymes are present within each in-vitro biological system (Brandon et al. 2003; Weisbrod et al. 2009). Another important consideration is the ease of preparation of each in-vitro assay system, as some assay systems are more challenging to prepare. Two of the more common in-vitro assay systems that are beginning to be used more frequently in fish biotransformation experiments include liver S9 subcellular fractions and fish hepatocytes. Liver S9 subcellular fractions are

prepared by centrifuging liver homogenate at 9000g to sediment cellular debris that is not needed (Weisbrod et al. 2009). This leaves the supernatant consisting of the cytosol and microsomal fractions. The microsomal fraction contains cellular membranes and endoplasmic reticulum which contain phase I biotransformation enzymes (i.e. cytochrome p450s) while the cytosolic portion contains phase II biotransformation enzymes (i.e. GSTs, SLTs) (Weisbrod et al. 2009). Important advantages to using this assay include the relative ease and cost effectiveness to prepare, the presence of phase I and II biotransformation enzymes, as well as the ability to maximize the use of limited tissues and resources with this method (Weisbrod et al. 2009). Weisbrod et al. (2009) have indicated that a 1 kg rainbow trout can produce enough liver S9 fractions to perform in-vitro biotransformation experiments for 10-50 chemicals. The relatively long storage time is also an advantage as well as it has been reported S9 subcellular fractions can be stored via cryopreservation for at least 2 years while maintaining initial enzyme activity (Johanning et al. 2012a). A potential disadvantage for the use of liver S9 fractions is that they may have lower enzyme activity compared to other in-vitro assay systems such as microsomes and cytosol (Brandon et al. 2003).

Freshly isolated fish hepatocytes consist of whole liver cells and provide advantages because they contain both phase I and II biotransformation enzymes and are relatively more comparable to a whole liver in-vivo (Brandon et al. 2003; Weisbrod et al. 2009). Furthermore, Mingoia et al. (2010) and Fay et al. (2014) have reported that cryopreserved hepatocytes provide similar metabolic capacity compared to fresh hepatocytes, which is another advantage. Another important advantage of fish hepatocytes are that because they are intact cells, they contain membrane transport processes such as efflux transporters that can influence the uptake and elimination of xenobiotics and their metabolites (Weisbrod et al. 2009). The major disadvantage with fish hepatocytes is that they can be relatively challenging to prepare compared to other in-vitro assay systems (Brandon et al. 2003; Weisbrod et al. 2009).

Comparisons of hepatic clearance obtained from fish liver S9 subcellular fractions and hepatocytes have also indicated that both assays provide similar measurements. Fay et al. (2017) reported that predicted in-vivo intrinsic clearance values obtained through cryopreserved hepatocytes yielded values that were within reasonable agreement when compared to in-vivo intrinsic clearance values obtained from liver S9 fractions for 5 of 6 chemicals and also resulted in the same rank order of activity of test chemicals. An OECD Ring Trial (2017) also reported similar results, reporting that in-vivo intrinsic clearance rates for multiple chemicals obtained

from both in-vitro systems were in good agreement (< 2-fold difference). These results suggest that either in-vitro assay system can be used for performing in-vitro biotransformation experiments to improve bioaccumulation assessment.

1.3 Biotransformation of xenobiotics

Biotransformation involves the action of enzymes converting chemicals into generally more polar water-soluble metabolites (Coecke et al. 2006). Biotransformation can not only influence the ability of a chemical to bioaccumulate, but it can also aid in the detoxification of the chemical, and in some cases, lead to chemical bioactivation (Brandon et al. 2003). The major organ where biotransformation generally occurs is the liver, however biotransformation can also occur in the kidneys, lungs, intestinal walls and contents, skin, blood-brain barrier and blood (Coecke et al. 2006). Biotransformation reactions of xenobiotics into more water-soluble metabolites are classified into phase I and phase II reactions, and biotransformation of a chemical can occur via one or the other, or a combination of both.

Phase I reactions are generally referred to as functionalization reactions, and consist primarily of oxidation (i.e. hydroxylation, deamination), reduction and hydrolysis reactions (i.e. ester and amide bond cleavage), with the main effect of making lipophilic molecules more polar and more readily excreted via the kidneys (Gibson and Skett 1986; Coecke et al. 2006). This is often achieved through the addition of a functional group (i.e. -OH, -SH, -COOH) to ultimately make the molecule more polar (Di Giulio and Hinton 2008; Gibson and Skett 1986). The majority of Phase I oxidation reactions are performed by the cytochrome P450 (CYP) family of enzymes. CYP enzymes occur in many isoforms and are the most abundant metabolizing enzymes in the liver. They have very broad substrate specificities, making them ideal for metabolizing a wide range of molecules (Coecke et al. 2006; Di Giulio and Hinton 2008; Crespi 1995). CYP enzymes are located in the smooth endoplasmic reticulum of the liver, although CYP activity also occurs in gastrointestinal mucosal cells, kidney, lung and skin (Di Giulio and Hinton 2008).

Phase II metabolic reactions consist of conjugation reactions of xenobiotics with endogenous cofactors (Cedarbaum 2015). Common cofactors include glucuronic acid, sulfate, glutathione and acetate (Cedarbaum 2015). Phase II enzymes can conjugate parent compounds in the absence of phase I metabolism, while products from Phase I reactions can

also be conjugated to make the metabolites even more polar and easier to excrete (Cedarbaum 2015; Di Giulio and Hinton 2008). The majority of Phase II metabolising enzymes are transferases, which include UDP-glucuronosyltransferases (UGTs), sulfotransferases (SULTs), N-acetyltransferases (NATs), and glutathione S-transferases (GSTs) (Anzenbacher and Anzenbacherova 2001; Coecke at al. 2006). The primary Phase II metabolic reactions which lead to detoxification of parent compounds involve glucuronide conjugation via UGTs, as it has been reported that in humans 40-70% of clinical drugs undergo glucuronidation reactions (Anzenbacher and Anzenbacherova 2001; Di Giulio and Hinton 2008). As with CYP enzymes, UGT proteins are distributed broadly throughout various tissues, with the liver being the primary location with the greatest abundance (Anzenbacher and Anzenbacherova 2001; Di Giulio and Hinton 2008).

Xenobiotic biotransformation in fish and mammals occurs via similar Phase I and Phase II metabolic reactions (Kleinow et al. 1987). Research in fish is more limited than that in mammals, although multiple CYP forms present in mammals appear to be present in fishes as well, with the greatest abundance occurring in the liver (Uno et al. 2012). In particular, CYP1, CYP2, and CYP3 families are prevalent in xenobiotic metabolism in fishes (Di Giulio and Hinton 2008).

Despite the similarities between biotransformation mechanisms in fish and mammals, differences exist regarding the metabolic handling of chemicals (Kleinow et al. 1987). Differences in reaction rates and products formed, as well as differences in the relative metabolic pathways are factors that contribute to differences between biotransformation mechanisms in fish and mammals (Kleinow et al. 1987). For instance, it has been reported that monooxygenation, which is one of the first steps in converting a chemical into a more water-soluble form, is a much slower process in fish than in rats and humans (Weisbrod et al. 2009). Because of this, compounds that are readily metabolized in rats and humans would be slowly metabolized in fish, leading to bioaccumulation in fish but not in rats, as was the case with 3,3,4,4-tetrachlorobiphenyl (PCB-77) (Jordan and Feely 1999; Weisbrod et al. 2009). Han et al. (2007) also reported that hepatocytes isolated from rainbow trout metabolized xenobiotics 5.5 to 78.5 fold more slowly than hepatocytes isolated from rats. Han et al. (2007) noted the biggest difference for atrazine with regard to xenobiotic metabolism, as the intrinsic clearance of atrazine in isolated rat hepatocytes was 3.81 ±1.96 ml/h for 10^6 cells and 0.002 ml/h for 10^6 cells in trout hepatocytes. The difference in metabolic activity between the different species could be

attributed to the lower activity of certain biotransformation enzymes in fish hepatocytes (Nabb et al. 2006).

Furthermore, interspecies differences in fish xenobiotic metabolism have been noted. Schultz and Hayton (1999) reported a 35-fold difference in intrinsic metabolic clearance of trifluralin between various species of fishes. Funari et al. (1987) also noted differences in monooxygenase activity and cytochrome P450 activity across various species of fish. Thus, there is a potential for wide variations in biotransformation capabilities of xenobiotics between different species of fish (Schultz and Hayton 1999). Due to the variation in biotransformation capabilities in different fish species, this represents a current limitation to IVIVE, as much of the in-vivo derived data are based on different fish species than are what are most commonly used to prepare in-vitro assay systems, making it difficult to draw conclusions when determining biotransformation and bioaccumulation potential of xenobiotics.

1.4 Enzyme kinetics in *in-vitro* biotransformation rates

Michaelis-Menten kinetics is the fundamental model for describing the kinetics of enzymes. Equation 1 describes a basic reaction occurring through an enzyme converting substrate to product. The initial reaction between enzyme (E) and substrate (A) forms an enzyme substrate complex (EA) and through a catalytic step (k_2) product (P) is formed.

$$E + A \leftrightarrow EA \overset{k_2}{\rightarrow} E + P \quad (1)$$

A key assumption of Michaelis-Menten kinetics is that the catalytic step (k_2) is much slower than the formation or deformation step such that the formation of the enzyme substrate complex is essentially at equilibrium (Rogers and Gibson 2009). Equation 2 describes the general Michaelis-Menten equation:

$$V = \frac{V_{MAX}\,[S]}{K_M + [S]} \quad (2)$$

where V is the rate of metabolite formed, [S] is substrate concentration, V_{MAX} is the maximum speed at which a certain amount of enzyme can catalyze a reaction, and K_M is the Michaelis constant, which is the substrate concentration required by for an enzyme to reach half of its

V_{MAX}. This equation describes how at low substrate concentrations (assuming a fixed amount of enzyme), reaction rate is going to increase linearly with increasing substrate concentration, as there are enough enzyme molecules to catalyze reactions, whereas as substrate concentrations increase, enzymes become saturated and the V_{MAX} is approached (Berg et al. 2002; Bisswanger 2008). With in-vitro biotransformation assays, it is often presumed that the starting substrate concentration be much lower than the K_M, such that the biotransformation rates obtained from these assays are well below enzyme saturation (Han et al. 2007, 2009; Nichols et al. 2013b; Johanning et al. 2012). This presumption is especially important in accurately determining biotransformation rates used to assess bioconcentration factors in fish, as Lo et al. (2015a) showed that the current convention for in vitro biotransformation studies which use 1.0 uM starting substrate concentration may be too high, leading to an underestimation of the in-vitro biotransformation potential and overestimation of bioconcentration factors of chemicals.

The Michaelis-Menten equation describes the formation of a metabolite(s), but in the case of most chemicals, the exact products and metabolic pathways along with the analytical tools required to analyze them are unknown. A rewritten form of the Michaelis Menten equation has been described by Obach and Reed-Hagen (2002) which measures substrate depletion and is shown in Equation 3:

$$k_{dep} = k_{dep,([S]=0)} \left(1 - \frac{[S]}{[S] + K_M} \right) \quad (3)$$

where k_{dep} is the in-vitro depletion rate, $k_{dep,([S]=0)}$ is the theoretical k_{dep} at an infinitesimally low substrate concentration, [S] is substrate concentration, and K_M is the Michaelis constant (Obach and Reed-Hagen 2002). Nath and Watkins (2006) showed through simulations that monitoring substrate depletion in this manner yielded comparable kinetic results when compared to the traditional product formation approach (Equation 2), assuming that one substrate, one enzyme and one metabolite were involved in the reaction.

1.5 Research Objectives

The overall objectives of this project was to:

1) Conduct in vitro substrate depletion experiments to determine in-vitro biotransformation rate constants of selected test chemicals

2) Perform IVIVE using two models to assess whole organism biotransformation rates (k_{MET}) and BCFs in fish
3) Compare k_{MET} and BCFs that are derived by IVIVE to similar in-vitro studies in the literature as well as *in-vivo* derived k_{MET} and BCFs

To accomplish this, *in-vitro* biotransformation rate experiments of test chemicals using rainbow trout liver S9 fractions were completed. As described earlier hepatocytes and liver S9 fractions are both useful assay systems for performing in-vitro biotransformation experiments to improve bioaccumulation assessment and provide similar results, however rainbow trout (*Oncorhynchus mykiss*) liver S9 subcellular fractions were used in this study because they are relatively easy to prepare and use, and also because they contain cytosolic and microsomal enzymes, which means they contain Phase I and Phase II metabolic enzymes that are responsible for metabolizing drugs and xenobiotics (Brandon et al. 2003; Weisbrod et al. 2009; Johanning et al. 2012a). Furthermore, because the specific metabolic pathway was unknown for three of the four chemicals in this study, the use of liver S9 fractions still provided an appropriate method to measure hepatic clearance (Johanning et al. 2012a). The test chemicals in this experiment were pyrene, cyclohexyl salicylate, methoxychlor, and 2,6-dimethyldecane. Their high log K_{ow} values (>4), along with their use in various BCF studies (e.g. Fay, HESI 2016; Laue et al. 2014; Lo et al. 2015a,b; other literature data) were the main purpose for using these chemicals. There were also in-vivo studies using these test chemicals from the Gobas Lab (DiMauro, in preparation; Lo et al. (2015b)), which allowed for a comparison to empirical data.

The *in-vitro* depletion rate constants obtained from the S9 *in-vitro* assays were then input into 2 different *in-vitro-in-vivo* extrapolation (IVIVE) models to extrapolate a whole-organism biotransformation rate constant (k_{MET}). The first IVIVE model was developed by Nichols et al. (2013), and was based on calculating hepatic clearance using a well stirred liver model to interconvert clearance and rate constants throughout the extrapolation process. This model also required an estimation of the apparent volume of distribution to obtain k_{MET} values, and also required various parameters such as hepatic blood flow, fraction of unbound chemical in blood, and blood–water partition coefficients. The second IVIVE was recently developed by Lee et al. (2017) and provided advantages in that it did not require interconversions between clearance and rate constants and instead relied on extrapolation of rate constants, and also involved easily measurable values during the preparations of S9 fractions and during in-vitro substrate depletion experiments (Lee et al. 2017). Knowledge of hepatic blood flow was not required as well with the Lee et al. (2017) IVIVE model.

The k_{MET} from the two IVIVE models were then input into a fish bioaccumulation model (Arnot and Gobas 2004) to estimate corresponding BCF values for each test chemical in fish. These extrapolated whole-organism biotransformation rate constants and BCFs for each test chemical were then compared to biotransformation rate constants and BCFs derived from complementary *in-vivo* experiments in the Gobas lab and *in-vivo* literature data. This also allowed for a comparison of the performance of the recently developed Lee et al. (2017) IVIVE model to the Nichols IVIVE model that had also been used in these in-vitro biotransformation studies.

Materials and Methods

2.1 Chemicals

Test chemicals pyrene and methoychlor were purchased from Sigma, cyclohexyl salicylate was purchased from Vigon International, and 2,6 dimethyldecane was purchased from ChemSampCo. Chrysene d-12 was purchased from Isotec. Chemical purities were all >98%. Acetonitrile, hexane, toluene, potassium hydroxide (KOH), and potassium phosphate (monobasic) (KH_2PO_4) were purchased from Caledon. Acetone and potassium phosphate (dibasic) (K_2HPO_4) were purchased from Anachemia, and potassium chloride (KCl) was purchased from EMD.

2.2 Fish

One batch of S9 (n=1) was made using a male rainbow trout (*Oncorhynchus mykiss*), which weighed approximately 1500g. Fish were obtained from Miracle Springs hatchery (Mission, BC). The fish was held in a flow through tank supplied with dechlorinated city water, held under natural light conditions, and were fed commercial 3 mm EWOS Pacific pellets (Surrey, BC) daily for at least 2 weeks. Fish were held at water temperatures of approximately $15^0C \pm 1^0C$.

2.3 Preparation of S9 Sub-Cellular Fractions

Liver S9 sub-cellular fraction preparation procedures followed the methods outlined by Johanning et al. (2012), with a few modifications. To begin S9 preparation rainbow trout were

humanely euthanized using 300 mg/L tricaine methanesulphonate (MS-222) and 300 mg/L sodium bicarbonate ($NaHCO_3$) (EMD) in dechlorinated water. Exposure to this concentration of MS-222 is not expected to have a significant effect on cytochrome p450 activity in rainbow trout (Kolanczyk et al., 2003). Following euthanasia, incisions exposing the internal organs were performed. The hepatic portal vein was perfused using a peristaltic pump at a rate of 9 ml/min., with one side of a tube with a needle attached to the end inserted into the portal vein, and the other side of the tube in a solution of ice-cold clearing buffer (Hanks Balance Salt Solution (HBSS without Ca^{+2} and Mg^{+2}) supplemented with 4.2 mM $NaHCO_3$, 2.3 mM ethylenediaminetetraacetic acid (EDTA, dibasic) (BioShop), and 1 M HEPES (BioShop), at a pH of 7.8). Perfusion of the liver was performed to ensure the S9 fractions did not contain blood borne metabolizing enzymes (Johanning et al., 2012). All instruments used during the perfusion process were chilled on ice. The livers were then excised, rinsed with ice-cold homogenization buffer (0.2 M phosphate buffer containing 1.15% KCl, at a pH of 7.4) and weighed. The weight of the liver in the preparation was 23.4 g. The liver was then minced on an ice-cold Kimax petri dish using a razor blade. The minced liver was then homogenized using a Potter-Elvehjem tissue homogenizer with Teflon tipped pestle (Kimble tissue grind comp, size 22; Vineland, NJ, USA) and glass mortar (Kimble tissue grind tube, size 24; Vineland, NJ, USA) on ice in one volume (g/mL) of homogenization buffer (0.2 M phosphate buffer containing 1.15% KCl, at a pH of 7.4). The VWR Canlab homogenizer (West Chester, PA, USA) was set at an approximate speed of 800 r.p.m., and the homogenizing process involved approximately seven passes. The homogenate was then transferred to 50 mL Oakridge centrifuge tubes (Nalgene Labware; Rochester, NY, USA), balanced, capped, and centrifuged (Hermle Model Z 360 K; Wehingen, BW, Germany) at 9000g for 20 minutes at 4^0C. Following centrifugation, the top lipid layer was discarded carefully via aspiration, and the remaining S9 fractions were aliquoted to 0.5 mL polymerase chain reaction (PCR) tubes (Axygen; Union City, CA, USA) and stored at -80^0C (Sanyo V.I.P. series -86^0C; Moriguchi, Osaka, Japan) until the day of incubations.

2.4 Incubations

Parallel incubations involving pyrene and test chemical were carried out in triplicate (n=3). Negative control incubations with each test chemical were also performed consisting of inactivated liver S9 and phosphate buffer. Inactivation of liver S9 was achieved through pre-incubating liver S9 at room temperature for 24 hours, followed by omission of NADPH from the incubation medium. The incubations for each test chemical had the same general procedure,

with volumes of components added to the subsampling incubation vial being altered depending on the test chemical. This was completed to improve chemical analysis using an Agilent 6890 gas chromatograph (GC) coupled to an Agilent 5973 mass spectrometer (MS). Pyrene was selected as a benchmark compound in this study due to a well-known understanding of its metabolic pathway (Kennedy et al., 1991; Namdari 1994). Pyrene has a relatively high log K_{OW}, and has often been in *in-vitro* biotransformation rate studies (Lo et al. 2015a).

2.4. General incubation procedure

Incubations were completed in triplicate, with the test chemical incubation and a pyrene incubation being run simultaneously using active S9. Prior to the start of the incubation the S9 fraction was pre-incubated in the water bath for 5 minutes to ensure thawing. The subsampling incubation vial was set-up such that the final protein concentration of S9 in the incubation vial was 1 mg/mL (Johanning et al., 2012), and the final concentration of β-NADPH (Sigma-Aldrich) in the incubation vial was 2 mM (Johanning et al., 2012). Spiking solutions containing the test chemical were made in different solvents depending on the test chemical, and were then used to add the test chemical to the incubation vial to achieve the desired starting concentration of test chemical. The final spiking solvent concentration in the incubation mixture was less than 0.5% (v/v). Incubation vials included phosphate buffer (0.2 M, pH 7.4), β-NADPH (Sigma-Aldrich), S9 fraction and test chemical. Refer to Table 2.1. for full details regarding the volumes for each incubation. The incubations were conducted in a water bath (Grant OLS 200) in unison with a cooling unit (CS 200G) at 13.50C. The vials were constantly shaken (60 r.p.m.) for the length of the incubation period. The incubation vial was immediately vortexed for 10 seconds, and the reaction was initiated immediately after. Subsampling incubation mixtures were introduced into either 2 mL amber autosampler vials (Agilent; Mississauga, ON, Canada) or 20 mL scintillation vials. 2 mL scintillation vials were used for methoxychlor, pyrene, and 2,6 dimethyldecane incubations because aliquots from the incubation mixture for each time point were sufficient for analysis via GC/MS. 20 mL scintillation vials were used for cyclohexyl salicylate incubations to increase the aliquot volumes for each time point to allow for adequate chemical analysis using the GC/MS. Depending on the test chemical, aliquots from the incubation vial were taken at varying time intervals throughout the reaction and added to a clean amber autosampler vial containing 200 µL of ice-cold acetonitrile (ACN) to terminate the reaction, followed by addition of 1 mL hexane. Chrysene d-12 (diluted in hexane) was added as an internal standard (final concentration of chrysene d-12 varied depending on the test

chemical). Full incubation details for each test chemical can found in Table 2-1. The samples were vortexed for 10 minutes at setting #10 (SIP ® vortex mixer, Baxter Scientific Products, USA), followed by a 10-minute centrifugation (Centra CL2 bench top centrifuge, Thermo IEC, USA) at 3.0 r.p.m. The hexane supernatant was then transferred to a clean amber autosampler vial for analysis via GC/MS.

Table 2.1. Overview of incubation details for each test chemical.

Test Chemical	Initial Substrate Concentration (μM)	S9 Protein conc. (mg/mL)	Sampling Time Points (min.)	Total volume of incubation (μL)	Volume of K-PO4 buffer added (μL)	Stopping Solution Volume (μL)	Extraction Solvent (μL)
Pyrene[a]	0.5	1.0					
Methoxychlor			0,15,30,45,60,75,90	1600	1127	Cold ACN, 200	Hexane, 1000
Cyclohexyl Salicylate			0,5,10,15,20,25	2500	1786		
2,6 Dimethyldecane	1.0		0,17.5, 35, 52.5, 70, 87.5[b] 0, 10, 20, 30, 40, 50[b]	1600	1128		Hexane, 600

[a] Incubation details for pyrene are not shown here because pyrene was run alongside the other test chemicals, and thus the exact experimental details for each pyrene run varied with each test chemical

[b] One incubation was run for 87.5 minutes, while the remaining two incubations were run for 50 minutes.

2.5 Chemical Analysis via GC/MS

The extract obtained from the incubations were analyzed using an Agilent 6890 gas chromatograph (GC) coupled to an Agilent 5973 mass spectrometer (MS) (Agilent, Mississauga, ON, Canada), and the GC had a cool on column injection port. The injection volume was 1 uL. There were two columns on which the chemicals were separated: a HP-5MS 5% phenyl methyl siloxane-coated column (30m x 0.25mm inner diameter, 0.25mm film thickness), and this column was connected to a 5m x 530µm x 0.25µm fused silica deactivated guard column (Agilent, Mississauga, ON, Canada). The carrier gas was helium, and the flow rate was 1ml/min. The oven temperature program was similar for pyrene, methoxychlor, and cyclohexyl salicylate. The initial injection temperature was 50^0C for pyrene (45^0C for methoxychlor and cyclohexyl salicylate), followed by a temperature ramp of 25^0C/min. to a max temperature of 290^0C. MS measurements were completed using 70 eV ion energy, and an ion source temperature of 230^0C. For 2,6 dimethyldecane, the initial injection temperature was 50^oC for 90 seconds, followed by a temperature ramp of 20^oC/min., followed by another temperature ramp of 25^oC/min. to a max temperature of 295^oC. The chemicals were quantified at select ions: m/z 202 for pyrene, m/z 227 for methoxychlor, m/z 120 for cyclohexyl salicylate, m/z 57 for 2,6 dimethyldecane and m/z 240 for chrysene d-12.

2.5.1. Calibration Standards

An internal standard (chrysene d-12) was added to each incubation vial to account for any changes in GC/MS responses and any variation in volume of extraction solvent added across vials. A calibration curve was also constructed for each test chemical at the time of incubation. Linear regression from the calibration curve was used to determine the concentration of the test chemical as a function of the relative peak area ratio of test chemical to internal standard. Using this peak area ratio, the linear regression was in the form y=mx+b, with the peak area ratio representing y, and x representing the chemical concentration. Rearranging of the equation to solve for x yielded the chemical concentration.

2.6 Extraction Efficiency Tests

Extraction efficiency tests were carried out for each test chemical prior to incubations to determine if correction factors had to be applied to the data when determining chemical

concentrations. A subsample incubation vial under no-cofactor control conditions was used. The concentrations of the test chemical in determining extraction efficiency was the same as that in incubations. Also, S9 concentration (1 mg/mL) and phosphate buffer were the same as that in incubations. The mixture was vortexed for 10 seconds, followed by transferring three aliquots from the incubation vial (n=3) to clean 2 mL autosampler vials containing 200 µL ice-cold acetonitrile. 1 mL of hexane was added to each vial, and then the extraction procedure involving shaking on the vortex mixer and centrifugation were identical to the incubation procedure (see 2.4). The supernatant was transferred to a clean 2 mL autosampler vial, followed by addition of chrysene d-12 (final concentration varied depending on concentration used for each test chemical incubation) for analysis with GC/MS. Test chemicals with the same concentration as was subsampled from the incubation vial, along with chrysene d-12 (same concentrations as that used in incubations), were added to hexane, and these served as representative of 100% extraction efficiency (n=3). Extraction efficiency of pyrene, methoxychlor, and cyclohexyl salicylate were essentially 100% (SD for pyrene, cyclohexyl salicylate and methoxychlor= 10%, 10%, 15% respectively) as they didn't differ significantly from the hexane standards, while the extraction efficiency for 2,6 dimethyldecane was 50% (SD=3%).

2.7 Protein Content Determination

The protein content of the S9 subcellular fractions was determined using the Bradford protein assay (Bradford 1976). A standard curve was constructed using bovine serum albumin (Sigma-Aldrich) at concentrations of 0, 0.01, 0.02, 0.04, 0.06, 0.08 mg/mL. The BSA standard curve stock solutions were initially made in autosampler vials containing BSA and phosphate buffer (0.2 M, pH 7.4) to a final volume of 1000 µL. This was followed by pipetting 50 µL of each standard into a 96 well plate with 200 µL of diluted Bradford reagent (diluted 1/5 in Ultrapure water: 8 mL of Bradford reagent in 40 mL of Ultrapure water) in triplicate (n=3). Johanning et al. (2012a) found average pooled protein S9 content to be approximately 26 mg/mL (CV=5%). Due to this, S9 dilution concentrations (0.04 – 0.08 mg/mL) were selected assuming that S9 has a protein content between 20-30 mg/mL when diluted 1:1 in buffer during the liver S9 preparation, as was the case in this study (Johanning et al. 2012a). The S9 dilution samples were also made initially in autosampler vials containing volumes of the S9 as well as phosphate buffer (0.2 M, pH 7.4) to a final volume of 1250 µL. 50 µL of each S9 dilution along with 200 µL of Bradford reagent were then added to the well plate in triplicate (n=3). The mean protein concentration of each S9 dilution sample was then determined using the equation of the line from the standard

curve, and then adjusted for volume and amount added accordingly to determine the actual protein content of each S9 dilution sample. Absorbance values of the BSA standards and liver S9 samples at a wavelength of 595 nm were determined using a Pharmacia LKB Ultrospec III UV/Vis spectrophotometer (Creve Coeur, MO, USA). Full details can be found in Appendix B.

2.8 Data and Statistical Analysis

The rate of depletion of the parent chemical during the incubation as a result of biotransformation was measured over time. The natural logarithm of the substrate concentration in the active S9/inactive S9 was plotted over time and the slope of this relationship was the first-order substrate depletion rate according to:

$$k_{\mathrm{dep}} = \frac{ln\left(\frac{C_{ACTIVE\ S9}}{C_{INACTIVE\ S9}}\right)}{t} \quad (4)$$

where k_{dep} is the first order depletion rate constant (1/min), t is incubation time and $C_{ACTIVE\ S9}$ and $C_{INACTIVE\ S9}$ were the substrate concentration in the active S9 incubation and substrate concentration in the inactive S9 incubations respectively. Linear regression analysis using Excel was completed to assess for significant differences in test chemical incubations for active and inactive S9 ($p<0.05$). All other statistical analyses were completed with JMP 12 (2016).

2.9 IVIVE Methods

Two IVIVE modelling procedures were tested in this study: one developed by Lee et al. (2017), and the Nichols et al. (2013a) model. The Nichols et al. (2013a) IVIVE modelling procedure was an updated IVIVE model. Briefly, the *in-vitro* intrinsic clearance ($CL_{IN\ VITRO,INT}$; mL/h/mg protein) was multiplied by the S9 content of liver tissue (mg/g liver) and the liver weight as a fraction of total body weight (g liver/g fish) to obtain the *in-vivo* intrinsic clearance ($CL_{IN\ VIVO,INT}$; mL/h/g fish). The hepatic clearance rate (CL_H) was calculated based on a well stirred liver model obtained from Wilkinson and Shand (1975) (Nichols et al. 2013a). The CL_H was then used to calculate the *in-vivo* biotransformation rate (k_{MET}), which was then used to predict BCF values. The Nichols et al. (2013a) IVIVE model incorporated the fish bioaccumulation model described by Arnot and Gobas (2004) when predicting BCF values. Full model details can be found in Nichols et al. (2013a). Model parameters are provided in the Appendix.

The Nichols et al. (2013a) model is based on estimating hepatic clearance as a function of hepatic blood flow similar to pharmaceutical methods, and to do this, estimates of parameters such as cardiac output, fraction of blood flow through the liver, and volume of distribution are required. However these measurements may not be readily available. Lee at el. (2017) presented an IVIVE approach that can estimate in vivo biotransformation rates from in vitro first order depletion rate constants without the need for interconversions to hepatic clearance. The Lee et al. (2017) IVIVE model follows a similar simplified approach that is better suited to bioaccumulation testing but is extrapolated to fish (Lo et al., in preparation). The major assumption for this method is that the liver is the main site of biotransformation in the body of the fish. Full model details can be found in Lo et al. (in preparation). Briefly, it involves estimating the maximum in vitro biotransformation rate constant through substrate depletion experiments, followed by normalizing of the maximum in vitro biotransformation rate constant to the fraction of unbound chemical in the incubation medium according to:

$$k^{*}_{\mathrm{dep,C\rightarrow 0}} = \frac{k_{\mathrm{dep,C\rightarrow 0}}}{f_{\mathrm{u,inc}}} \quad (5)$$

where $k^{*}_{\mathrm{dep,C\rightarrow 0}}$ is the normalized biotransformation rate constant, $k_{\mathrm{dep,C\rightarrow 0}}$ is the biotransformation rate constant, and $f_{\mathrm{u,inc}}$ is the fraction unbound in the incubation medium. The in vivo hepatic biotransformation rate constant was then estimated through a scaling factor and the fraction unbound in the liver according to:

$$k_{\mathrm{MET,H}} = k^{*}_{\mathrm{dep,C\rightarrow 0}} \cdot SF \cdot f_{\mathrm{u,H}} \quad (6)$$

where $k_{\mathrm{MET,H}}$ is the in vivo hepatic biotransformation rate constant, *SF* is the scaling factor, and $f_{\mathrm{u,H}}$ is the fraction unbound in the liver. This was followed by an estimation of the whole organism biotransformation rate constant (k_{MET})according to:

$$k_{\mathrm{MET}} = k_{MET,H} \cdot \frac{M_H}{M_B} \quad (7)$$

where M_H and M_B are the masses of the chemical in the liver and in the whole organism (including the liver), respectively. This was assuming the liver is the main site of biotransformation, and that the rate of distribution of the chemical between tissues is fast and

the chemical in the liver is in near equilibrium with the rest of the organism. After calculation of k_{MET}, k_{MET} values were normalized to the weight of the fish according to equation 8:

$$k_{MET,10g} = k_{MET} (10/W_B)^{-0.25} \quad (8)$$

where W_B is the wet weight of the fish (g). This allometric scaling relationship was derived from Arnot et al. (2008), who observed that smaller fish had higher biotransformation rates constants than larger fish, and used an exponent of -0.25 to normalize the biotransformation rate constant to a 10 g fish. $k_{MET, 10g}$ values were then input into the Arnot and Gobas fish bioaccumulation model to obtain BCFs.

Results and Discussion

3.1 Calibration Curves

Calibration curves for pyrene, methoxychlor, cyclohexyl salicylate, and 2,6 dimethyldecane are displayed in Appendix A. The calibration curves illustrate the concentration ranges suitable for GC/MS analysis. R^2 values were greater than 0.97 for all calibration curves.

3.2 Rainbow Trout (*Oncorhynchus mykiss*) Liver S9 Protein Content

The mean protein content of the rainbow trout (*Oncorhynchus mykiss*) liver S9 batch used for all of the incubations was determined to be 24.45 ± 2.07 mg protein/ mL S9 (mean ± SD). S9 concentrations were diluted such that they were in the linear range of a standard curve made using bovine serum albumin (BSA). The R^2 of the BSA standard curve was 0.9692. The standard curve and the dilution calculations can be found in Appendix B.

3.3 *In-Vitro* Substrate Depletion Experiments

Results from the in-vitro substrate depletion experiments can be found in Table 3.1. and Figures 3.1., 3.2., and 3.3. Slopes for active and inactive S9 samples with each test chemical were obtained from linear regression ($p<0.05$). There was no significant loss of any of the test chemicals in the inactive S9 control treatment incubations ($p>0.05$). Concentrations of methoxychlor and 2,6 dimethyldecane inactive S9 showed an increase throughout the incubation period. In-vitro depletion rate constants for each test chemical (k_{dep}; min^{-1}) were derived from the slope of the regression line obtained from the ratio of remaining test chemical concentration in the active S9 to the remaining test chemical concentration in the inactive S9 over time.

k_{dep} pyrene results are provided in Table 3.1. and are displayed in Figures 3.1., 3.2., and 3.3. Pyrene incubations (n=9) were conducted alongside each test chemical and pyrene k_{dep} values incubated alongside each test chemical were also compared with each other to assess if there were significant differences between the pyrene incubations. The mean k_{dep} of pyrene

conducted in parallel with methoxychlor was 0.020 ± 0.001 min^{-1}, the mean k_{dep} of pyene conducted in parallel with cyclohexyl salicylate was 0.029 ± 0.002 min^{-1}, while the mean k_{dep} of pyrene conducted in parallel with 2,6 dimethyldecane was 0.011 ± 0.001 min^{-1} (mean ± standard error of the mean (SEM)). The means were significantly different from each other when compared using ANOVA test (p=0.0006), and a Tukey's Honestly Significant Difference (HSD) test revealed significant differences between pyrene depletion rates obtained from the three sets of pyrene incubations. Pyrene depletion rates obtained from incubations run alongside methoxychlor and cyclohexyl salicylate differed significantly (p<0.0127). Pyrene depletion rates incubated alongside 2,6 dimethyldecane differed significantly from those obtained in methoxychlor incubations (p<0.0209) and cyclohexyl salicylate (p<0.0005) as well. The mean pyrene depletion rate constant (n=9) from all pyrene incubations was 0.023 ± 0.003 min^{-1} (mean ± SEM). The use of pyrene as a reference compound to conduct parallel S9 incubations with each test chemical was useful because the difference in pyrene rates indicated a potential difference in S9 activity among S9 batches. By gaining more information about S9 activity of the S9 through the use of reference compounds, it could help to characterize the variability that may be evident between different S9 batches.

The results from the methoxychlor substrate depletion experiments (n=3) are displayed in Figure 3.1. and Table 3.1., with the corresponding pyrene incubations results ran in parallel displayed as well. Linear regression was performed to determine the depletion of methoxychlor and pyrene over time. Methoxychlor depletion rate constants (k_{dep}; $min.^{-1}$) were on average lower than pyrene depletion rate constants (Table 3.1.) despite having similar starting substrate concentrations. This indicates that biotransformation of methoxychlor was slower than pyrene. Linear regression analysis also indicated biotransformation was occurring, as p-values were 0.009, 0.002, and 0.011 for each of the incubations. The mean in vitro depletion rate constant of methoxychlor was determined to be 0.017 ± 0.001 $min.^{-1}$ (mean ± SEM).

Cyclohexyl salicylate depletion experiments (n=3) are displayed in Figure 3.2. and depletion rate constants in Table 3.1., along with the corresponding pyrene depletion curves that were run side by side at the same starting chemical concentration (0.5 µM). Linear regression was used to determine the biotransformation of both test chemicals over time. Regression analysis indicated that biotransformation was occurring, as p-values were 0.001, 0.002, and 0.001 for each of the incubations. The mean k_{dep} value of cyclohexyl salicylate incubations was 0.204 ± 0.063 min^{-1} (mean ± SEM) and was higher than the k_{dep} of pyrene.

There was some variability in the k_{dep} value of the cyclohexyl salicylate replicate 2 results, as the k_{dep} value obtained from this incubation was more than double the k_{dep} obtained from the other two incubations.

2,6 dimethyldecane depletion curves along with the corresponding pyrene depletion curves are displayed in Figure 3.3. 2,6 dimethyldecane incubations proceeded with a starting concentration of 1.0 µM to improve detection of the chemical using GC/MS analysis, while pyrene was run at 0.5 µM. Linear regression was used to plot the extent of biotransformation of each chemical. Regression analysis of active S9 incubations indicated that biotransformation did not occur in incubation 1 (p=0.5) and incubation 3 (p=0.236), although biotransformation did occur in incubation 2 (p=0.03). These results in incubation 1 and 3 may be due to the variability that was observed during the extraction procedure for 2,6 dimethyldecane, and is discussed further in Section 3.6. Despite regression analysis not providing a statistically significant depletion rate constant in these incubations, depletion rate constants were still used as inputs to IVIVE modeling and BCF estimations. It should also be noted that pyrene k_{dep} values obtained in these incubations were lower when compared to the pyrene k_{dep} values obtained from cyclohexyl salicylate and methoxychlor incubations, indicating that S9 activity was lower when running these incubations than incubations ran previously for methoxychlor and cyclohexyl salicylate.

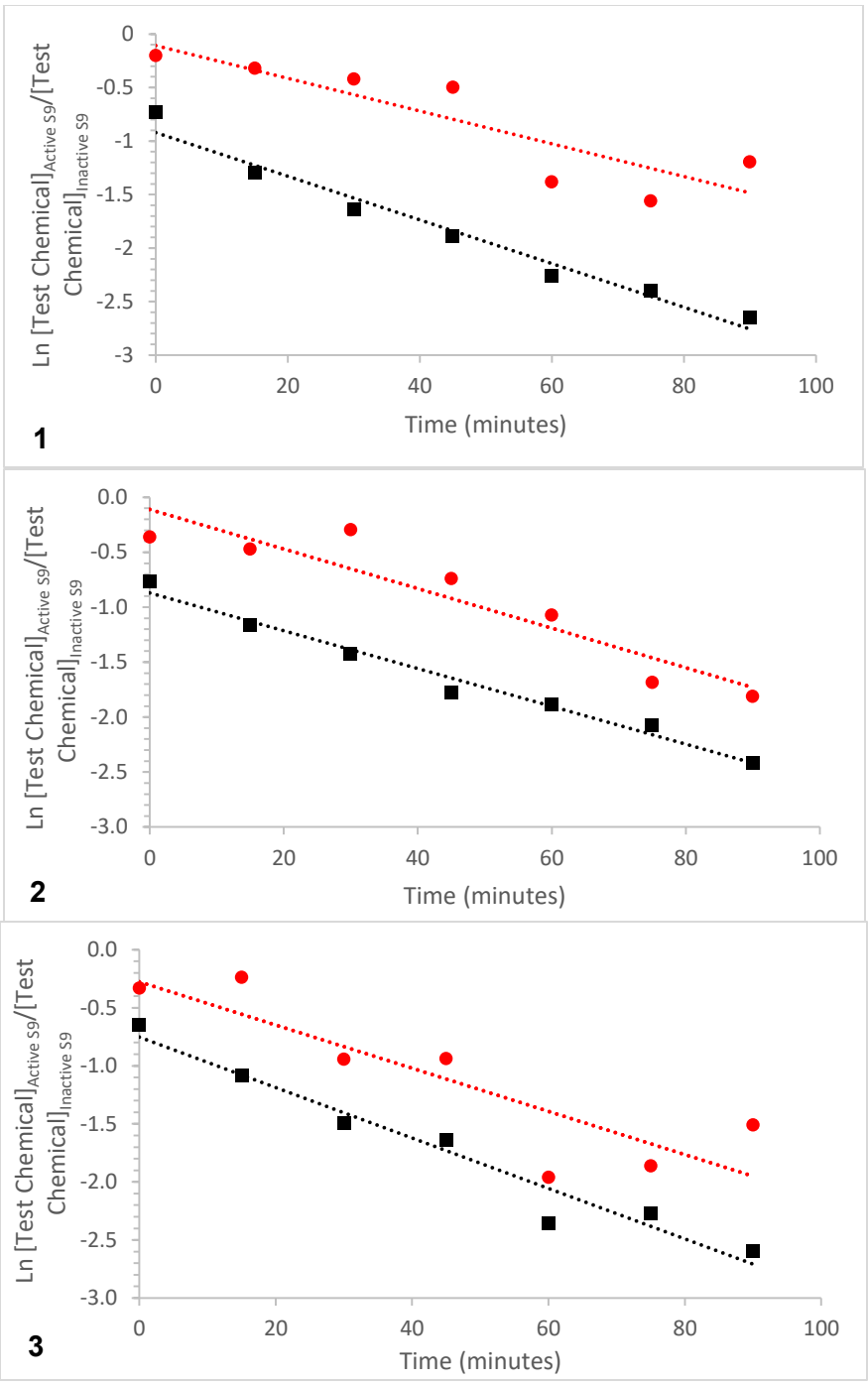

Figure 3.1. **Biotransformation of methoxychlor and pyrene over time (minutes) by rainbow trout (*Oncorhynchus mykiss*) active liver S9 fractions. The natural logarithm of the ratio of remaining concentration in active S9/inactive S9 over time is displayed, and initial substrate concentration was 0.5 µM. Methoxychlor is shown in red (●) and parallel pyrene incubations in black (■). Results from three incubations are shown (1,2,3).**

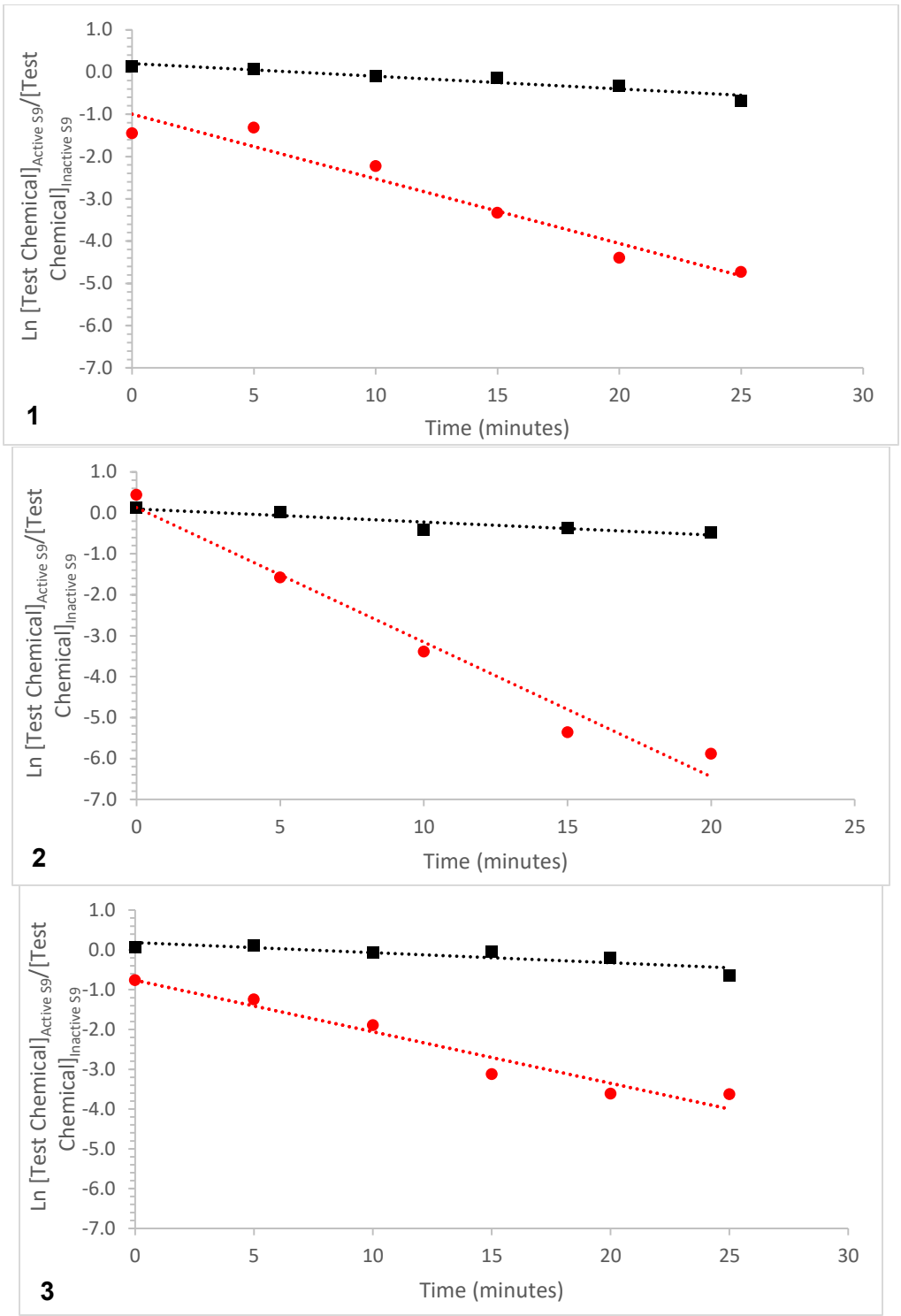

Figure 3.2. Biotransformation of cyclohexyl salicylate and pyrene over time (minutes) by rainbow trout (*Oncorhynchus mykiss*) active liver S9 fractions. The natural logarithm of the ratio of remaining concentration in active S9/inactive S9 over time is displayed, and initial substrate concentration was 0.5 µM. Cyclohexyl salicylate is shown in red (●) and parallel pyrene incubations in black (■). Results from three incubations are shown (1,2,3).

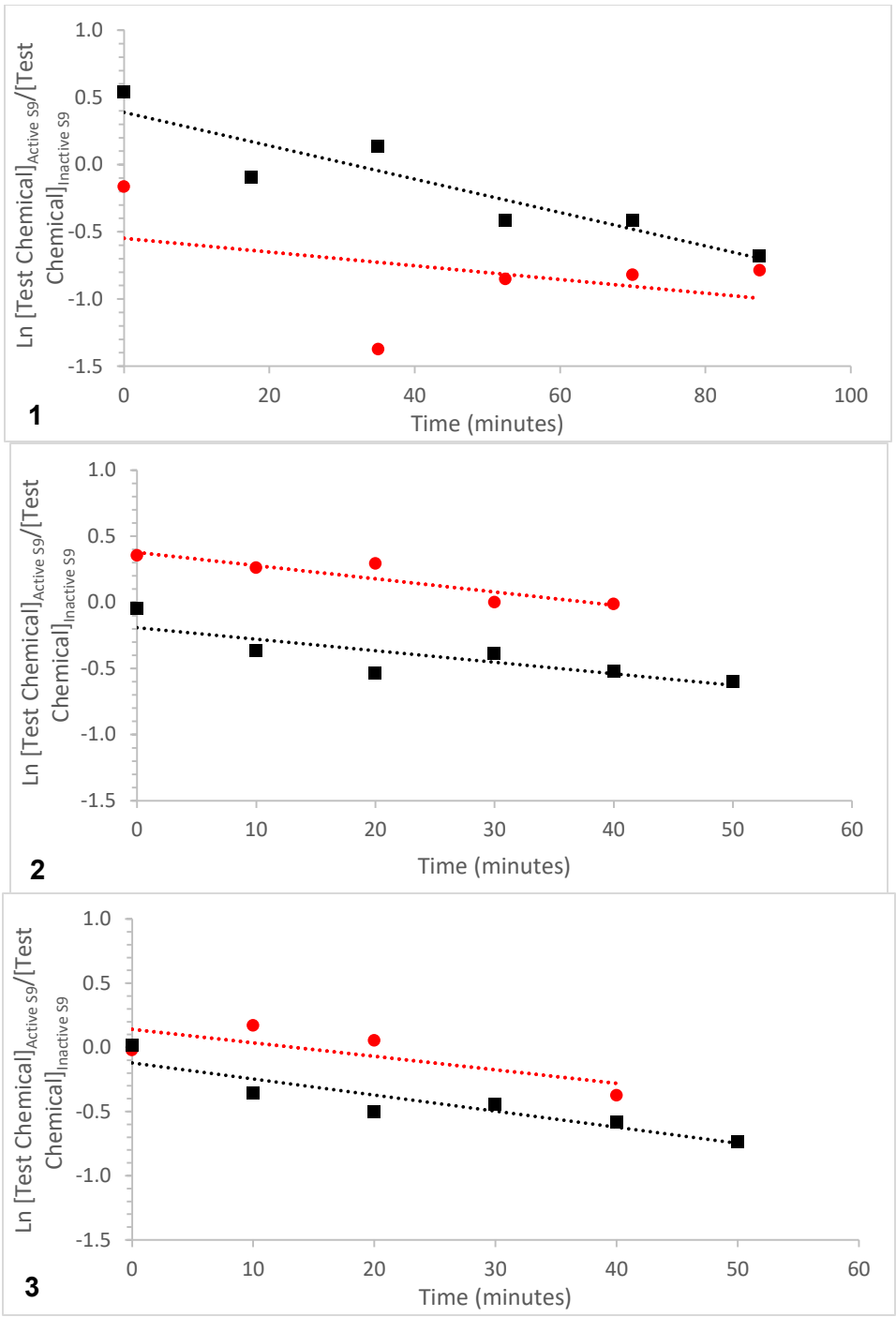

Figure 3.3. **Biotransformation of 2,6 dimethyldecane (DMD) and pyrene over time (min.) by rainbow trout (*Oncorhynchus mykiss*) active liver S9 fractions. The natural logarithm of the ratio of remaining concentration in active S9/inactive S9 over time is displayed, and initial substrate concentration of 2,6 DMD was 1.0 µM and 0.5 µM for pyrene. 2,6 DMD is shown in red (●) and parallel pyrene incubations in black (■). Results from three incubations are shown (1,2,3). Incubation 1 was performed for 90 minutes, while incubations 2 and 3 were performed for 50 min.**

Table 3.1. in-vitro substrate depletion rates (k_{dep}; minutes^{-1}) of pyrene, methoxychlor (MC), cyclohexyl salicylate (CS), and 2,6 dimethyldecane (2,6 DMD). Parallel pyrene experiments were conducted alongside each of the test chemicals, and the corresponding test chemical is indicated in brackets. The natural logarithm of remaining substrate concentration in active S9/inactive S9 was plotted vs time, and a linear regression was performed to obtain a slope. The mean k_{dep} is displayed with the standard error of the mean in brackets. MC, CS, and 2,6 DMD depletion rates were normalized to each pyrene depletion rate with the standard error (relative error x k_{dep} test chemical/k_{dep} pyrene) displayed in brackets.

Substrate	Initial Substrate Conc. (µM)	Depletion rate constant (k_{dep}; min^{-1})	Depletion rate normalized to pyrene depletion rate (k_{dep}; min^{-1})
Pyrene			
Replicate 1 (Methoxychlor)	0.5	0.020	
Replicate 2 (Methoxychlor)	0.5	0.017	
Replicate 3 (Methoxychlor)	0.5	0.022	
Replicate 4 (CS)	0.5	0.030	
Replicate 5 (CS)	0.5	0.032	
Replicate 6 (CS)	0.5	0.025	
Replicate 7 (2,6 DMD)	0.5	0.012	
Replicate 8 (2,6 DMD)	0.5	0.009	
Replicate 9 (2,6 DMD)	0.5	0.013	
MEAN		0.023 (0.003)	
Methoxychlor			
Replicate 1	0.5	0.015	0.75 (0.19)
Replicate 2	0.5	0.018	1.05 (0.19)
Replicate 3	0.5	0.019	0.86 (0.23)
MEAN		0.017 (0.001)	
Cyclohexyl Salicylate			
Replicate 1	0.5	0.153	5.07 (1.02)
Replicate 2	0.5	0.329	10.3 (2.88)
Replicate 3	0.5	0.130	5.10 (1.61)
MEAN		0.204 (0.063)	
2,6 Dimethyldecane			
Replicate 1	1.0	0.005	0.41 (0.55)
Replicate 2	1.0	0.010	1.14 (0.49)
Replicate 3	1.0	0.011	0.84 (0.53)
MEAN		0.009 (0.001)	

3.4 Intra lab comparison of in-vitro intrinsic clearance rates ($Cl_{in\ vitro,\ INT}$) of pyrene

A comparison of mean $Cl_{IN\ VITRO,\ INT}$ (ml/h/mg protein) pyrene values obtained from various studies conducted in the Gobas Lab at approximately 0.5 µM pyrene starting substrate concentration is shown in Figure 3.4., while a similar comparison of mean pyrene k_{dep} values from the Gobas Lab are displayed in Figure 3.5. Mean k_{dep} (hr^{-1}) of pyrene across the various studies ranged between 0.92 ± 0.21 to 2.76 ± 0.94 (mean ±SD), while the average coefficient of variation between the studies was 28.2%, and ranged from 21.0% to 40.8%. Similar results were also obtained when comparing $Cl_{IN\ VITRO,\ INT}$. $Cl_{IN\ VITRO,\ INT}$ was determined by dividing the k_{dep} by the protein content in the incubation. Mean $Cl_{IN\ VITRO,\ INT}$ (ml/h/mg protein) of pyrene ranged from 0.21 ± 0.04 (mean ± SD) to 1.20 ± 0.49 (mean ± SD). To better characterize the variability between the studies the coefficient of variation was determined for each study (i.e. 100 × standard deviation/ average value; CV). The average CV across all studies was 28.1%, and ranged from 19.6% to 40.8%. These results indicate that normalizing to protein content doesn't reduce the variability when comparing biotransformation rates across studies. Similar results were obtained from an OECD Ring Trial study as well, as they reported mean inter-laboratory CV of $Cl_{IN\ VITRO,\ INT}$ (ml/h/mg protein) pyrene values between 5 S9 batches to be 26.5% (SD = 10.9%, range from 16.3% to 38.9%). Variation between the different S9 batches may have been attributed to enzyme recovery in S9 fractions, differences in investigator handling during preparation of S9 fractions, as well as differences in fish body size conditions.

Incomplete recovery of metabolizing enzymes during S9 preparation from the various studies compared to the intact tissue could have been a contributing factor that influenced biotransformation rates and subsequent *in-vitro* intrinsic clearance rates (Nichols et al. 2006). Schultz and Hayton (1999) reported that *N*-depropylase activity varied 35-60% in liver S10 fractions from fish. Differences between recovery of metabolizing enzymes within the S9 batches may have been due to investigator handling during the S9 preparation (Johanning et al. 2012b; Fay et al. 2017). Johanning et al. (2012b) reported intra-lab variation of k_{dep} for decanol to be 2.57 ± 1.59 hr^{-1} (mean ± SD) and suggested that differences in S9 preparation and handling by investigators to be a contributing factor. Although enzyme activity was not measured in this study, it has been recommended that enzyme assays that can characterize the S9 batches' Phase I and Phase II activity be conducted to assess the metabolic potential (Johanning et al. 2012a). In this study, pyrene was incubated alongside each of the test

chemicals to characterize the S9 activity of the batch. Examples of enzyme assays to measure Phase I activity involve CYP1A activity toward 7-ethoxyresorufin (EROD), while enzyme assays to measure Phase II activity involve the conjugation of 1-chloro-2,4-dinitrobenzene by glutathione S-transferase (GST) and glucuronidation of p-nitrophenol by UDP-glucuronyltransferase (UGT) (Han et al. 2009).

Differences in fish weights also may have influenced the variation in *in-vitro* intrinsic clearance rates across the different studies. Rainbow trout used in S9 preparations across the different studies in the Gobas Lab varied between 160g-1500g. To date, allometric scaling and its influence on Phase I and Phase II activity of S9 fractions has yet to be studied (Nichols et al. 2013a; Fay et al.2017). However, intraspecific metabolic rate (measured as resting oxygen consumption) on a whole animal basis has shown to be scaled to a fractional exponent of body weight, ranging between 0.6-0.9 (Nichols et al. 2013a; Franklin et al. 1995; Ohlberger et al. 2012). Allometric relationships that contain similar exponents relating fish size to various biological factors such as chemical flux and cardiac output have also been included in published chemical fish accumulation models (Nichols et al. 2013a). An investigation to further understand the effects of fish body weights on Phase I and Phase II metabolic activity in S9 fractions should be conducted. This could help characterize some of the potential intra-lab and inter-lab variation that exists when comparing biotransformation potential of hydrophobic chemicals from various batches of S9 prepared from different fish body sizes.

A potential method to address the variability in enzyme viability and metabolic capacity across different batches of S9 could be to use a benchmark compound run in parallel with the test chemical during substrate depletion experiments. Guomao et al. (2016) investigated using benzo-a-pyrene as a benchmark compound to normalize the variation in biotransformation rates across difference batches of analyses by normalizing the *in-vitro* intrinsic clearance of the test chemical to the intrinsic clearance of benzo-a-pyrene. Guomao et al. (2016) reported phenanthrene (PH), 6-methoxy-tetrabromodiphenyl ether (6-MeO-BDE47), and 4-nonylphenol (4-NP) intrinsic clearance values (mL/h/mg of protein) were 0.007 ± 0.0017, 0.027 ± 0.005, and 0.021 ± 0.013 (±SD) with the variation (% CV) in intrinsic clearance values being 23%, 23%, and 61%, respectively. After normalizing each chemical's intrinsic clearance value with benzo-a-pyrene's intrinsic clearance value, the intrinsic clearance for PH, 6-MeO-BDE47, and 4-NP were 0.22 ± 0.037, 0.41 ± 0.019, and 0.29 ± 0.046 (± SD) respectively, and the CV of intrinsic clearance values across different batches for the three compounds decreased to 5−17%.

Incorporation of a benchmarking compound helped to substantially reduce the variability between different batches in their study. In this study, pyrene was run in parallel with methoxychlor, cyclohexyl salicylate and 2,6 dimethyldecane with the intention of using this same benchmarking method to better compare data across different batches of S9 from other studies, but there were no other studies that incorporated this method. It could be useful to include a benchmark compound when performing substrate depletion experiments to determine biotransformation rates of specific test chemicals as normalizing to the benchmark chemical can potentially help to reduce the variability of biotransformation rates of test chemicals evident across different batches of S9.

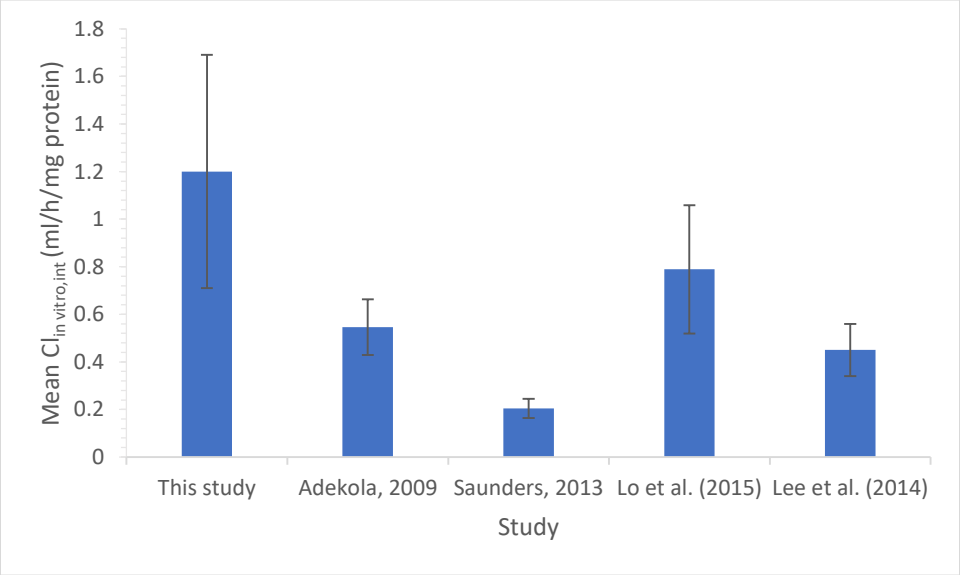

Figure 3.4. Comparison of mean pyrene $CL_{IN\ VITRO,\ INT}$ (ml/h/mg protein) values obtained from various studies conducted in the Gobas Lab at approximately 0.5 µM pyrene starting substrate concentration (Adekola, 2009 was 0.54 µM while Lo et al. (2015) was 0.56 µM pyrene). Error bars are the standard deviation.

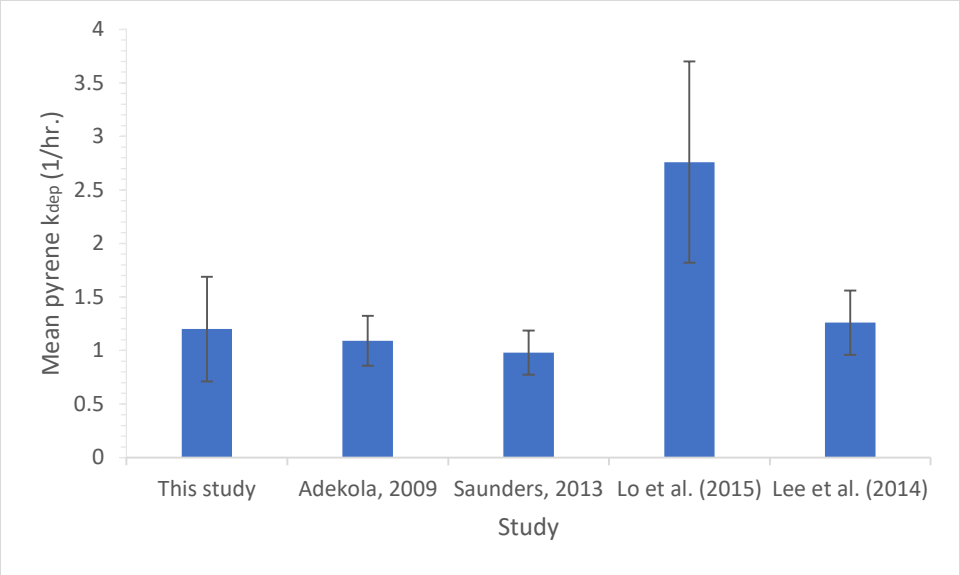

Figure 3.5. Comparison of mean pyrene k_{dep} (hours^{-1}) values obtained from various studies conducted in the Gobas Lab at approximately 0.5 µM pyrene starting substrate concentration (Adekola, 2009 was 0.54 µM while Lo et al. (2015) was 0.56 µM pyrene). Error bars are the standard deviation.

3.5 Estimation of modelled k_{MET} and BCF values

Whole organism biotransformation rate constants (k_{MET}; d^{-1}) were determined using the Lee et al. (2017) IVIVE as well as the Nichols et al. (2013a) model, and were then compared to in-vivo k_{MET} values obtained from complimentary studies conducted within the Gobas lab from DiMauro (in preparation) and Lo et al. (2015b) (see Table 3.2.). In-vivo k_{MET} values were also normalized according to equation 8 (refer to Material and Methods) to a 10 g fish weight to allow for better comparisons between in-vitro derived k_{MET} values and in-vivo derived k_{MET} values. The k_{MET} estimates were then input into a fish bioaccumulation model (Arnot and Gobas 2004) to estimate BCFs (Table 3.3.). When extrapolating using the Nichols et al. (2013a) model, BCF and k_{MET} data was modelled under two binding assumptions (f_u): a) f_u=calc: ratio of free chemical fractions *in-vivo* in blood plasma and *in-vitro* in the S9 fraction and b) f_u=1: equal availability of test chemical to biotransformation enzymes *in-vivo* and *in-vitro*. Furthermore, the Nichols et al. (2013a) IVIVE model and the parameters in the model were based on the standardized size of fish used in in-vivo experiments (10 g fish with 5% lipid content). The OECD Ring trial BCF data (OECD 2017) were also based on a standardized fish (10 g rainbow trout with 5% lipid content) for better comparison with OECD TG 305 BCF data. k_{MET} values of the 95% upper and lower confidence intervals of the mean k_{MET} for each test chemical were also

considered in model estimates to generate a range of k_{MET} and BCF values. Uncertainties in the model were not included in the calculations.

Table 3.2. provides an intra-lab comparison of k_{MET} values estimated using the depletion rate constants from *in-vitro* substrate depletion experiments input into the two IVIVE models described earlier compared to *in-vivo* derived k_{MET} estimates (pyrene, methoxychlor, and cyclohexyl salicylate in-vivo data obtained from DiMauro (in preparation) and 2,6 dimethyldecane data obtained from Lo et al. (2015b)). Figure 3-6 provides a graphical representation of the intra-lab comparison of k_{MET} values for pyrene, methoxychlor, cyclohexyl salicylate, and 2,6 dimethyldecane. Pyrene and methoxychlor k_{MET} values estimated using the Nichols IVIVE model when f_u was calculated showed good agreement with the *in-vivo* k_{MET} values (less than 1 fold difference). With the Nichols IVIVE model, k_{MET} values estimated assuming f_u=1 were 13.7 fold higher with respect to pyrene and 23.5 fold higher with respect to methoxychlor when compared to *in-vivo* derived k_{MET} values. Cyclohexyl salicylate k_{MET} values estimated using the Nichols IVIVE model when f_u was calculated was approximately 2.6 fold higher than the *in-vivo* derived k_{MET} estimates, while k_{MET} estimates assuming f_u=1 were approximately 6.1 fold higher than the respective *in-vivo* k_{MET} values.

Overall, k_{MET} values estimated using the Lee et al. (2017) IVIVE model were lower than k_{MET} values estimated using the Nichols et al. (2013a) model and *in-vivo* k_{MET} values. Estimated values for k_{MET} of pyrene using the Lee et al. (2017) IVIVE model were approximately 2 fold lower than the k_{MET} values estimated from the Nichols et al. (2013a) model (compared to f_u=calc. estimates because Lee et al. model doesn't assume f_u=1) and *in-vivo* derived k_{MET} estimates. k_{MET} values of methoxychlor estimated using this model followed a similar trend as well, as k_{MET} estimates were approximately 2 fold lower than k_{MET} values obtained from the Nichols et al. (2013a) model, but were in very reasonable agreement with *in-vivo* derived k_{MET} estimates. Cyclohexyl salicylate k_{MET} values obtained from using the Lee et al. (2017) model were higher and differed by approximately 2.2 fold compared to in-vivo data, but varied less than 1 fold compared to Nichols et al. (2013a) f_u=calc. estimates.

Table 3.3. provide BCF predictions after inputting k_{MET} values obtained from both IVIVE models into a fish bioaccumulation model (Arnot and Gobas 2004) for pyrene, methoxychlor, cyclohexyl salicylate, and 2,6 dimethyldecane. Figure 3.7. also provides a graphical representation of the same data for the four chemicals. These predicted BCFs were compared

to BCF predictions obtained from an OECD Ring trial as well as empirical BCF data. The OECD Ring trial results used to compare predicted BCFs also incorporated in vitro biotransformation rate constants into an IVIVE model to predict BCFs.

BCFs of pyrene estimated with the inclusion of modelled k_{MET} values were lower than BCFs assuming no biotransformation (k_{MET}=0) of pyrene. This indicates the importance of considering biotransformation in BCF predictions, as biotransformation can impact the bioaccumulation potential of chemicals. Pyrene BCFs obtained using the Lee et al. IVIVE model were less than 1 fold higher than BCFs obtained using the Nichols model assuming f_u=calc. BCF predictions using k_{MET} input from the Lee et al. IVIVE model also yielded approximately 3.8 fold higher BCFs than the highest *in-vivo* BCF study found in the literature. When comparing BCFs from this study to results from an OECD Ring Trial, the BCFs predicted using the Lee et al. IVIVE were approximately 5.8 fold higher than the f_u=calc. results from the OECD ring trial. The BCFs predicted with the Nichols IVIVE model were approximately 4 fold higher when assuming f_u=calc. compared to OECD Ring Trial BCF results, but were in reasonable agreement assuming f_u=1. Finally BCFs predicted using the Nichols IVIVE model were approximately 2.7 fold higher compared to empirical BCFs when assuming f_u=calc., and were within the range of empirical BCF values when comparing f_u=1 BCF estimates. Methoxychlor BCFs predicted with inclusion of k_{MET} values was also lower than BCFs predicted without biotransformation. Similar trends observed with the pyrene BCF comparisons were evident with methoxychlor as well. Lee et al. IVIVE BCF predictions were within reasonable agreement when compared to BCFs predicted using the Nichols IVIVE assuming f_u=calc. OECD ring trial results assuming f_u=calc. also were in good agreement compared to Lee et al. IVIVE BCF predictions. Nichols (2013) derived BCF predictions from this study under both binding assumptions were below the results from the OECD Ring Trial (approximately 1.8 fold lower under both binding assumptions). Overall, there was a large difference between modelled BCFs and empirical BCFs, but BCFs assuming f_u=1 yielded better comparisons than f_u=calc.. Cyclohexyl salicylate BCF predictions with consideration of k_{MET} were lower than BCF predictions without consideration of k_{MET}. When comparing BCFs from the Lee et al. IVIVE model with f_u=calc. BCF predictions from the Nichols et al. (2013a) model, there was approximately less than 1 fold difference. When comparing to results from the OECD Ring Trial, Lee et al. IVIVE predicted BCFs were in good agreement (< 1 fold difference), while Nichols model predictions were also in good agreement under both binding assumptions compared to OECD Ring Trial results. Modelled BCFs from both IVIVE models were also much lower when compared to the empirical

BCFs. Finally, 2,6 dimethyldecane BCF predictions with consideration of biotransformation were also much lower when compared to assuming no biotransformation. BCF predictions using Lee et al. IVIVE k_{MET} were in good agreement when compared to Nichols et al. BCF predictions, and Lee et al. BCF predictions were approximately 9 fold higher compared to empirical BCFs, while Nichols et al. BCF predictions assuming f_u=calc. was 5.8 fold higher compared to empirical BCFs. Nichols et al. BCF estimates assuming f_u=1 was approximately less than 2.7 fold lower compared to empirical BCFs as well.

Overall, comparisons of k_{MET} data between the two IVIVE models were in good agreement with each other (see Table 3.2.). This is especially promising regarding the use of the Lee et al. (2017) IVIVE model, as much of the parameters are easily measurable and don't require the use of literature derived values for input as the Nichols et al. (2013a) IVIVE model does. However, despite the potential usefulness of both IVIVE models, there was variation when comparing results to in-vivo derived k_{MET} values, indicating that the models must continue to be improved. Some of this variability may be due to the uncertainty within the extrapolation models, which are discussed below.

Estimated BCFs for all of the chemicals when considering biotransformation were lower than when biotransformation was assumed to be zero. Furthermore, comparison of these values to empirical BCFs were in better agreement than BCF estimates that assumed no metabolism, which was consistent with previous studies (Han et al. 2007, 2009; Cowan Ellsberry et al. 2008; Dyer et al. 2008; Laue et al. 2014). However, comparison of BCFs using k_{MET} values estimated using the Gobas Lab IVIVE were all higher when compared to estimated BCFs using k_{MET} values from the Nichols model for all three chemicals. This variability may be due to the uncertainty within the different extrapolation models, which are discussed below. Differing starting chemical concentrations may explain some of the variation between this study and the OECD Ring Trial. For instance, pyrene starting concentrations were approximately 20 times lower in the OECD Ring Trial (starting concentration=0.025μM) compared to this study (starting concentration=0.5μM). Overall, assuming that fish weights were matched up and similar IVIVE models were used, the results from this study when compared to previous in-vitro studies (OECD Ring Trial) were in reasonable agreement, and when compared to in-vivo BCFs were closer than assuming no metabolism (i.e. k_{MET}=0).

When using the Nichols IVIVE model to extrapolate k_{MET} and BCFs, it was completed under two binding assumptions, assuming f_u=calc. and f_u=1. The f_u=calc. assumption assumes the ratio of free chemical fractions in blood plasma to the in-vitro S9 system, while the f_u=1 assumption assumes that the test chemical is equally available to biotransformation enzymes in blood plasma and in-vitro S9 (Nichols et al. 2013a; Laue et al . 2014). The results from this study indicated that chemical binding influenced IVIVE, and that the influence varied with in vitro clearance. When in vitro clearance was high as was the case with cyclohexyl salicylate, blood flow to the liver limited the rate of hepatic clearance (which impacted BCF predictions as well) and made the modelled hepatic clearance values insensitive to errors in f_u. This impacted BCF results as well, as BCF predictions for cyclohexyl salicylate using f_u=1 were still lower than those predicted assuming f_u=calc. however the difference in predicted BCFs between the two binding assumptions was less than 2 fold. With slower metabolized compounds that exhibited lower rates of in vitro clearance such as methoxychlor, much larger differences in predicted BCFs were obtained when comparing the different binding assumptions. Similar results were obtained by Laue et al. (2014), who observed much higher differences in predicted BCFs between the two binding assumptions with slower metabolized compounds, and much smaller differences for quickly metabolized compounds. In another study Nichols et al. (2013b) used solid phase microextraction (SPME) to characterize binding of PAHs in S9 fractions and in solutions used to perfuse isolated trout livers. By using this method, Nichols et al. (2013b) directly compared chemical binding effects on IVIVE by measuring in vitro activity and then extrapolating to the intact liver and comparing to measured levels of hepatic clearance. They found that with well metabolized compounds, both binding assumptions provided good estimates of hepatic clearance (due to flow limitations), while slower metabolized compounds exhibited measured levels of clearance that were more accurate when compared to f_u=1. Fay et al. (2017) also found similar results when comparing hepatic clearance results from trout hepatocytes and liver S9 fractions, and found that when in vitro activity is high, hepatic clearances estimates were in good agreement under both binding assumptions.

At the moment, there isn't a mechanistic rationale that explains these findings or suggests using one binding assumption over the other when discussing the effect of chemical binding on hepatic clearance. Due to this, chemical binding on hepatic clearance in these extrapolations is a primary source of uncertainty in fish biotransformation extrapolations and further investigation is needed to characterize this (Nichols et al. 2013a, 2013b; Laue et al. 2014). The use of both binding assumptions when extrapolating biotransformation rates can still

be useful however as it can provide upper and lower limits of hepatic clearance and resulting BCF estimates, however this may not be ideal for slowly metabolized compounds due to the large difference between the two binding assumptions (Nichols et al. 2013a).

As mentioned earlier, there are limitations and sources of variation with the substrate depletion approach and taking in-vitro derived data and extrapolating it to compare to in-vivo data. Variation between different in-vitro biotransformation rate studies may be attributed to enzyme recovery in S9 fractions, differences in investigator handling during preparation of S9 fractions, as well as differences in fish body sizes used to prepare S9 fractions. One other potential source of error can be due to non-specific binding of hydrophobic chemicals to S9 or vials, which would decrease the bioavailability of the chemical, limiting its availability to the enzymes in the in-vitro system, leading to an underestimation of k_{MET} (Lee et al. 2014). This may have been one possible explanation for the results from the 2,6 dimethyldecane incubations in this study, and is discussed further in section 3.6. Furthermore, if BCFs are going to be used as evaluative measures of chemical bioaccumulation to assess the accuracy of IVIVE, uncertainty regarding the allometric scaling of biotransformation exists as well that has to be further investigated. In this study, in vitro biotransformation rates from substrate depletion experiments were input into IVIVE models to extrapolate k_{MET} values and subsequent BCF estimates along with upper and lower 95% confidence interval values for these values. It should be noted that when extrapolating from k_{dep} values to k_{MET} to BCF values, there is a degree of model error and uncertainty with the associated parameters and assumptions within these IVIVE models which are described below.

The Nichols et al. (2013a) IVIVE model includes parameters that are based on literature data unless they were actually measured in the lab and allowed for users to adjust values if needed. However because the parameters are based on literature data from previous experiments, the potential for variability within these parameters does exist (Han et al. 2009). Nichols et al. (2013a) performed a sensitivity analysis and found that the binding term (f_u) and the apparent volume of distribution ($V_{D,BL}$) were key parameters that influenced IVIVE. The influence of f_u and its effect on hepatic clearance has already been discussed above, and with the $V_{D,BL}$, which is based on the ratio of partitioning based BCF (BCF_P) and blood to water partition coefficient (P_{BW}), error is possible because it combines the error associated with these two values (Nichols et al. 2013a). k_{MET} values in this IVIVE model are based on the ratio of

hepatic clearance to the apparent volume of distribution, and thus uncertainties in these parameters can influence k_{MET} estimates.

Another source of variability arises with reported log K_{ow} values, as these can potentially vary within the literature. For instance, pyrene was reported to have log K_{OW} values ranging from 4.77 to 5.52, while methoxychlor K_{OW} values ranged from 4.68-5.08 (compiled in Mackay et al. 2006). Errors in log K_{ow} are a potential area of concern with regard to the Nichols model, as model results are strongly dependent on the hydrophobicity of the test chemical, which in turn can influence k_{MET} estimations (Nichols et al. 2013a). Furthermore, BCF predictions using the fish bioaccumulation model are also influenced by K_{OW}. At higher K_{OW}, the BCF becomes more sensitive to biotransformation because other rates of elimination are slower relative to lower K_{OW} where the opposite occurs (Arnot and Gobas 2006). Therefore BCF predictions can vary depending on the reported K_{OW} value that is used for a test chemical.

Another potential source of uncertainty is that the model assumes that the liver is the only site of biotransformation. This may not be the case, as other organs such as the intestines and the gills may influence biotransformation as well. In a study by Gomez et al. (2010), propranonol and ibuprofen predicted BCFs were reduced by trout gill biotransformation. Furthermore Lo et al. (2015b) reported that after dietary exposure, gastrointestinal biotransformation rate constants contributed more to overall biotransformation in fish than somatic biotransformation. Due to the potential for extrahepatic metabolism, current predictions of k_{MET} values from IVIVE models and BCF estimates which are based on hepatic biotransformation can only be considered a conservative estimate at this time.

Comparisons between in-vitro derived BCFs from rainbow trout and in-vivo derived BCFs from other fish species should also be taken with caution as well due to the potential variation between biotransformation from different species (Han et al., 2007). In vivo data from other fish species were used in this study when comparing to BCF estimates from rainbow trout S9 fractions due to the limited availability of data. However, studies have shown that enzyme activity varies across different fish species, which in turn can affect biotransformation (Forlin et al. 1995). The lack of reliable in-vivo biotransformation rate data also represents a barrier to validate and implement in vitro assays for measuring biotransformation rates (Lo et al. 2015a).

A recently developed IVIVE model developed by Lee et al. (2017) was also tested in this study. Despite the potential advantages to using this model which were discussed earlier, the model has only been used previously in fish studies once before, and potential uncertainties exist that can influence outputs from the model. In this study some of the parameters in the scaling factor calculation (i.e. volume of liver S9 fraction collected after centrifugation) were obtained from Lo et al. (in preparation) based on the similarities in S9 preparation procedures between the studies. These values were not measured in this study because at the time of S9 preparation the model hadn't been developed yet. This may have affected the subsequent results in this experiment. The model may also be sensitive to the unbound fractions of chemicals in the incubation mixture ($fu_{,inc}$) and in the liver ($fu_{,H}$). The fu_{inc}, can be calculated from previously derived relationships (Austin et al. 2002; Escher et al. 2011; Nichols et al. 2013b), estimated (Lo et al. in preparation) or measured with sorbent phase dosing (Escher et al. 2011). In this study, fu_{inc}. was estimated using the equation derived by Lo et al. (in preparation), however further investigation is needed to test this equation. This IVIVE model also assumes that the liver is the main site of biotransformation, however as mentioned earlier when discussing the Nichols IVIVE model, this may not necessarily be the case due to extrahepatic metabolism.

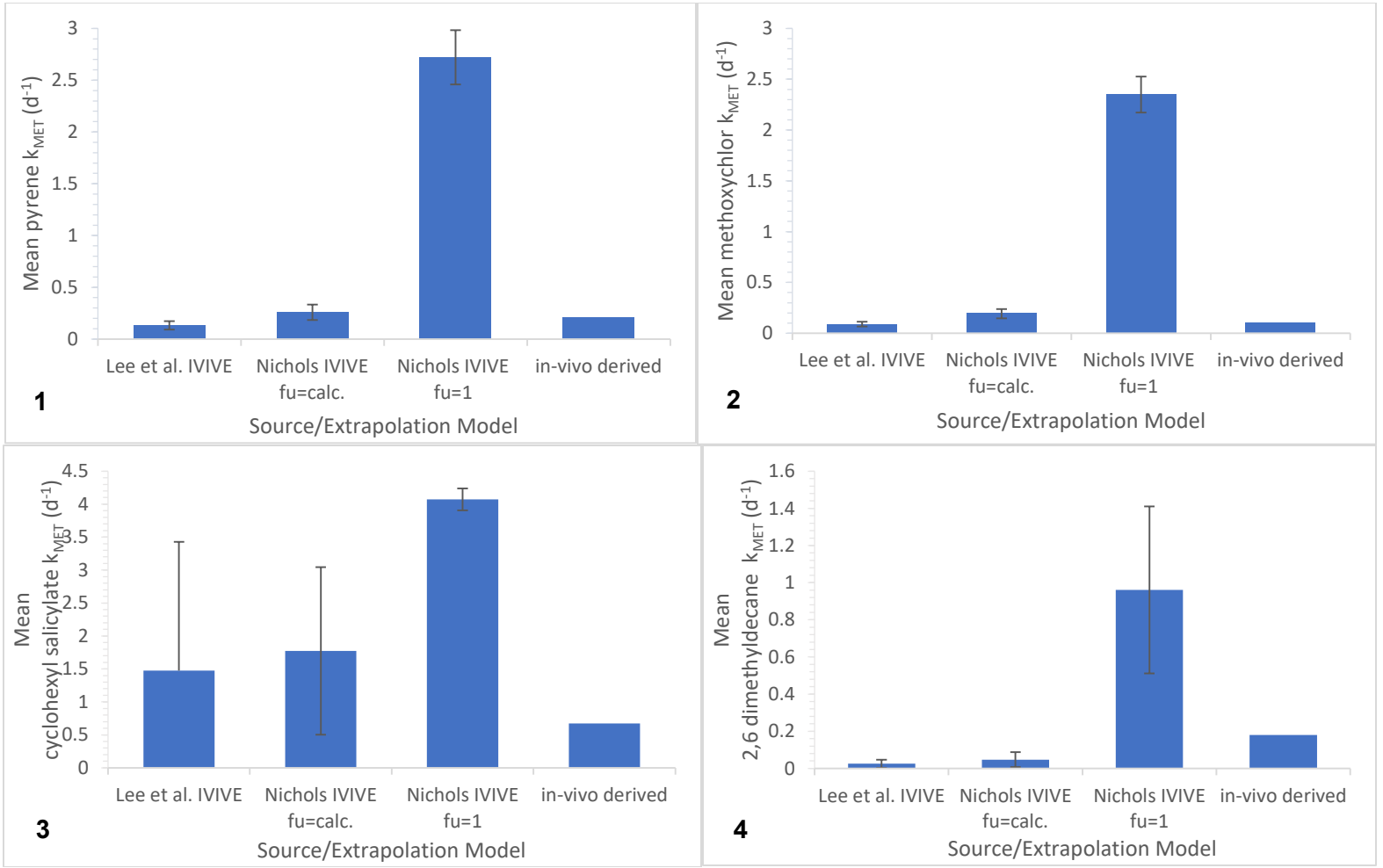

Figure 3.6. Intra-lab comparison of mean k_{MET} (d^{-1}) values obtained for pyrene (1), methoxychlor (2), cyclohexyl salicylate (3), and 2,6 dimethyldecane (4). Errors bars are the upper and lower 95% confidence intervals of the mean k_{MET}. in-vitro rates from this study were inputted into multiple IVIVE models to extrapolate k_{MET}, which were compared to complimentary in-vivo derived k_{MET} values from the Gobas Lab (in-vivo pyrene, methoxychlor, and cyclohexyl salicylate data obtained from DiMauro (in preparation), and 2,6 dimethyldecane in vivo data obtained from Lo et al. (2015)).

Table 3.2. Intra-lab comparison of in-vitro pyrene, methoxychlor, cyclohexyl salicylate, and 2,6 dimethyldecane mean k_{MET} (d^{-1}) values obtained in this study compared to in-vivo derived k_{MET} values obtained from complimentary studies in the Gobas Lab. Mean k_{MET} values estimated are displayed with upper and lower 95% confidence interval of mean k_{MET} values in brackets.

Chemical	Log K_{ow}	Mean k_{dep} (hr^{-1})	Mean k_{MET} (d^{-1}) Lee et al. (2016) IVIVE model	Mean k_{MET} (d^{-1}) Nichols et al. (2013) IVIVE model		*in-vivo* k_{MET} (d^{-1}) values
				f_u=calc.[a]	f_u=1[a]	
Pyrene	4.9	1.20	0.13 (0.09-0.17)	0.26 (0.18-0.33)	2.72 (2.46-2.98)	0.18[b]
Methoxychlor	5.1	1.04	0.09 (0.07-0.11)	0.19 (0.15-0.24)	2.35 (2.17-2.53)	0.10[b]
Cyclohexyl Salicylate	4.7	12.2	1.47 (3.43)	1.77 (0.50-3.04)	4.07 (3.90-4.24)	0.73[b]
2,6 Dimethyldecane	6.1	0.51	0.03 (0.003-0.05)	0.05 (0.007-0.09)	0.96 (0.51-1.41)	0.18[b]

[a] *in-vitro* k_{MET} values shown under 2 assumptions with regard to the binding term f_u: a) f_u=calc: ratio of free chemical fractions *in-vivo* in blood plasma and *in-vitro* in the S9 fraction and b) f_u=1: equal availability of test chemical to biotransformation enzymes *in-vivo* and *in-vitro*

[b] pyrene, methoxychlor, and cyclohexyl salicylate in-vivo data obtained from DiMauro (in preparation), and 2,6 dimethyldecane in-vivo data obtained from Lo et al. (2015b) dietary bioaccumulation study

Table 3.3. Comparison of pyrene, methoxychlor, cyclohexyl salicylate and 2,6 dimethyldecane BCF values (L/kg) obtained in this study compared to BCF data obtained in the literature. 95% confidence intervals of the mean k_{MET} extrapolated to BCFs are displayed in brackets. Empirical BCF values are the median value, with the lowest and highest BCF value found in the literature displayed in brackets.

Chemical	Log K_{ow}	IVIVE-BCF (k_{MET}= 0)	BCF Lee et al. 2017 IVIVE	BCF Nichols et al. 2013 IVIVE		OECD Ring Trial BCF[a]		Laue et al. 2014[b]		Empirical BCFs
				f_u=calc.	f_u=1	f_u=calc.	f_u=1	f_u=calc.	f_u=1	
Pyrene	4.9	3469	1958 (1724-2266)	1388 (1181-1682)	207 (189-227)	322	206			145 (97-484)
Methoxychlor	5.1	5441	2935 (2626-3329)	1940 (1682-2291)	236 (220-254)	3445	426			174
Cyclohexyl Salicylate	4.7	2261	351 (165)	299 (184-799)	140 (136-146)	463	182	312	140	600 (440-900)
2,6 Dimethyldecane	6.1	20673	8166 (5350-17176)	5295 (3240-14449)	343 (235-635)					910

[a] OECD Ring Trial starting chemical concentration of pyrene was 0.025 µM, methoxychlor was 0.32 µM, and cyclohexyl salicylate was 1.0 µM; BCFs predicted using Nichols et al. (2013a) IVIVE extrapolation model

[b] BCF values calculated using allometrically scaled $CL_{IN\ VIVO,INT}$, and the starting chemical concentration was 1.0 µM

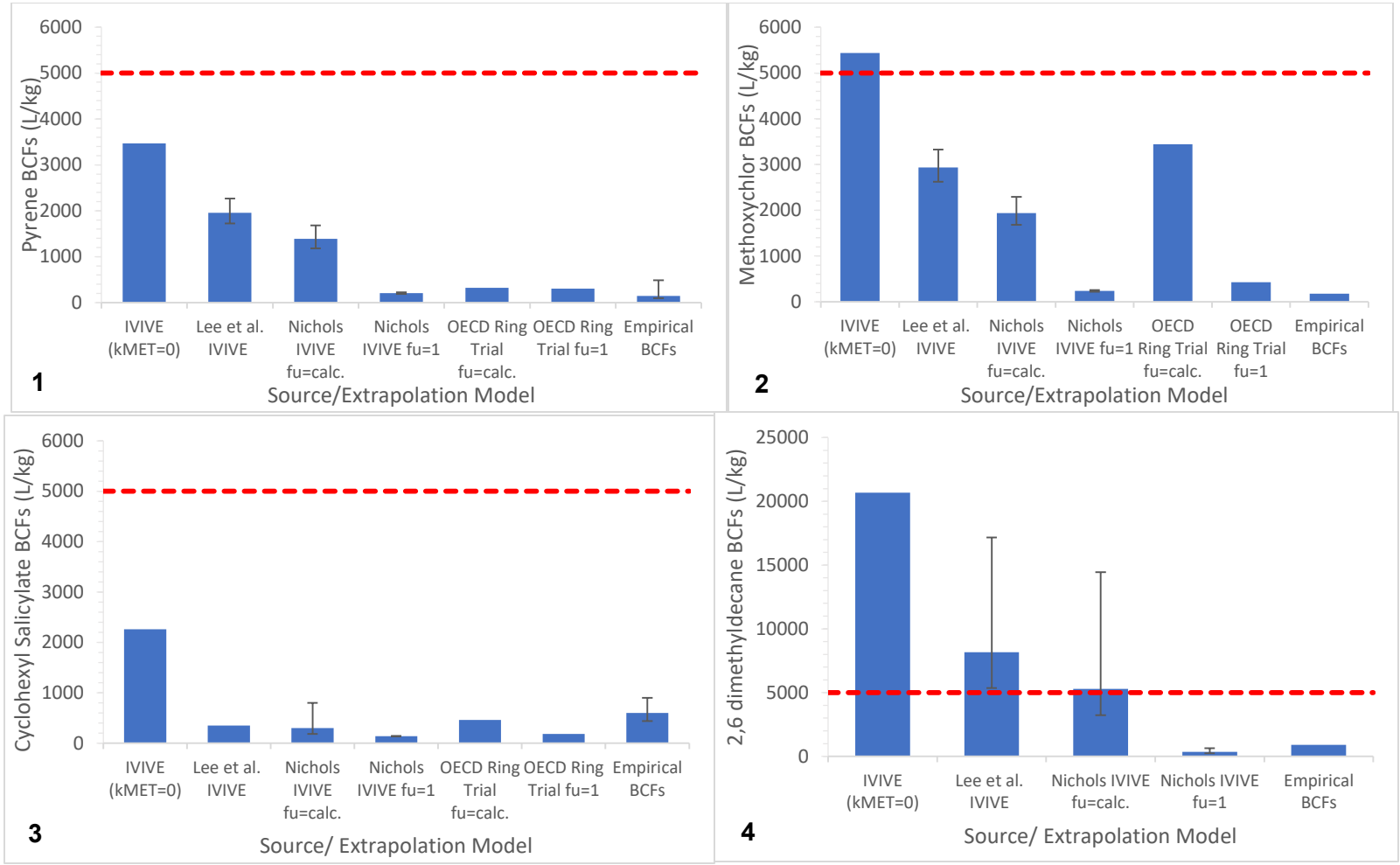

Figure 3.7. Comparison of modelled BCFs predicted using *in-vitro* k_{dep} values from this study with empirical BCFs and an OECD Ring Trial for pyrene (1), methoxychlor (2), cyclohexyl salicylate (3) and 2,6 dimethyldecane (4). The red dashed line is representative of the CEPA BCF bioaccumulation criteria. Error bars for the Lee et al. IVIVE and the Nichols IVIVE f_u=calc. and f_u=0 are the 95% confidence intervals of the mean k_{MET} extrapolated to BCFs. For the empirical BCFs, the median is shown for pyrene and cyclohexyl salicylate, with the error bars representing the lowest and the highest empirical BCF found in the literature.

3.6 2,6 Dimethyldecane Incubations

Table 5-2 provides k_{MET} estimates for 2,6 dimethyldecane along with in-vivo k_{MET} data from Lo et al. (2015b) for 2,6 dimethyldecane. When comparing k_{MET} data from this study obtained using the Lee et al. (2017) model, there was approx. a 6 fold difference compared to in-vivo results, but differences between k_{MET} obtained from the Lee et al. model compared to the Nichols et al. model were in good agreement. 2,6 dimethyldecane k_{MET} values estimated using the Nichols IVIVE model when f_u was calculated were approximately 3.5 fold lower compared to in-vivo k_{MET} values, and when f_u=1, k_{MET} was approximately 5 fold higher compared to in-vivo k_{MET}. The results from this study involving 2,6 dimethyldecane (2,6 DMD) indicated that 2,6 dimethyldecane biotransformation was much slower in in-vitro experiments than in-vivo experiments. Possible explanations for the lack of biotransformation of 2,6 DMD in this study may be related to non-specific binding of hydrophobic chemicals to S9 or vials, which would decrease the bioavailability of the chemical, limiting its availability to the enzymes in the in-vitro system, leading to an underestimation of the biotransformation rate.

The rate of the chemical for enzymes to act on it are crucial for the biotransformation, and this is related to the fraction unbound of the chemical (Trowell et al. 2018). Highly hydrophobic chemicals tend to have higher bioaccumulation potential due to their higher affinities for lipids, proteins or other biomolecules (Gulden and Seibert 2005; Heringa et al. 2003). In many cell based assays, large amounts of proteins are necessary as well, which could lead to high sorptive capacity between hydrophobic chemicals and proteins, ultimately leading to a decrease in the bioavailability of the chemical to be metabolised (Kwon et al. 2009; de Bruyn and Gobas 2007). To improve solubility of hydrophobic chemicals, the introduction of the chemical using a co-solvent is used. In this study, 2,6 DMD (log K_{OW}=6.1) was introduced to the S9 system by dissolving it in hexane spiking solvent. The issue with using a co-solvent is that it could lead to incomplete dissolution of the hydrophobic test chemical within the aqueous medium, reducing the bioavailability of the chemical and the subsequent biotransformation rate of the chemical (Kwon et al. 2009; Lee et al. 2014). This issue could potentially be overcome by using a solvent free dosing approach for highly hydrophobic chemicals such as 2,6 DMD. Lee et al. (2014) developed and implemented a solvent free dosing method by loading a test chemical into an ethylene vinyl acetate (EVA) thin film sorbent phase and then delivering the chemical into an S9 system by passive diffusion to determine in-vitro biotransformation rates of highly hydrophobic chemicals. Lee et al. (2014) reported that in-vitro biotransformation rates measured

using the thin film passive dosing system were 20 and 2 times higher for relatively highly hydrophobic chemicals chrysene (log K_{OW}=5.60) and benzo-a-pyrene (log K_{OW}=6.04) respectively when compared to biotransformation rates derived from spiking solvent delivery experiments. Another potential factor may have been the relatively high starting concentration used in 2,6 dimethyldecane (1.0 µM) in-vitro biotransformation incubations. As reported by Lo et al. (2015a), in-vitro biotransformation rates are dependant on the substrate concentration, as lower concentrations result in faster biotransformation rates, and thus lowering the concentration may also be beneficial, assuming 2,6 dimethyldecane can be detected via GC/MS at those lowered concentrations. Further investigation of the bioaccumulation potential of 2,6 DMD should be conducted using a solvent free dosing method along with lowering the starting substrate concentration to assess whether biotransformation of the chemical occurs faster in-vitro.

3.7 Future Directions

When comparing k_{MET} values and BCF results from in vitro depletion experiments in this study to corresponding data in the literature, results were in reasonable agreement, indicating the potential usefulness of in vitro depletion experiments in assessing the bioaccumulation potential of chemicals. However, the uncertainty regarding allometric scaling and its influence on biotransformation in fish, the uncertainty in the selection of values for f_u, as well as the unknown influence of extrahepatic metabolism indicate that current IVIVE modelling estimates should be considered a conservative assessment.

As mentioned earlier, current IVIVE modelling assumes that the liver is the main site of biotransformation without consideration for extrahepatic metabolism, increasing the uncertainty associated with IVIVE modelling estimates. Ramesh et al. (2004) showed that the intestines can contribute to first-pass metabolism of absorbed and ingested chemicals, while Lo et al. (2015b) demonstrated that biotransformation of hydrophobic chemicals occurred substantially in the intestines of fish. Furthermore, UDP-glucuronosyltransferase and glutathione-transferase, which are phase II enzymes have been shown to be active in rainbow trout gut subcellular fractions, another indication that biotransformation can occur outside the liver as well (Hanninen et al. 1987). This could potentially be an issue with hydrophobic chemicals due to the gastrointestinal tract being the primary route of exposure in natural settings (Nichols et al. 2009). Future studies should attempt to incorporate extrahepatic metabolism into IVIVE modelling when assessing the bioaccumulation potential of chemicals. With inclusion of extrahepatic metabolism it would likely

lead to estimated BCFs that are lower than when assuming hepatic metabolism only, and thus current BCF predictions based on in-vitro biotransformation should be considered a conservative estimate.

Overall, due to the uncertainty regarding BCFs predicted from in-vitro data and its ability to predict in-vivo bioaccumulation of chemicals, in-vitro substrate depletion experiments can be useful as a screening tool to determine if additional work with an in-vivo study is necessary when assessing the bioaccumulation potential of chemicals (Nichols et al. 2006). Inclusion of in-vitro derived data into a weight of evidence approach can also be useful as well to make a more informed and transparent evaluation of the bioaccumulation potential of chemicals (Nichols et al. 2009).

Conclusion

In conclusion, through the use of subcellular liver S9 fractions obtained from rainbow trout, in-vitro depletion rate constants were successfully determined for pyrene, methoxychlor, cyclohexyl salicylate and 2,6 dimethyldecane. In-vitro depletion rate constants were then input into two IVIVE models to determine in-vivo biotransformation rate constants to assess the performance of these IVIVE models. Comparison of k_{MET} values obtained from both IVIVE models were in reasonable agreement with each other, while comparisons of calculated k_{MET} using both IVIVE models were also in reasonable agreement when compared to in-vivo derived k_{MET} values for pyrene and methoxychlor. This indicates the potential usefulness of both IVIVE models for estimating k_{MET}, however further work is still needed to fine-tune the IVIVE models to allow for more accurate comparisons to in-vivo derived values. Also, more data is required using the IVIVE models as well due to the large variety of chemicals. Finally, estimated k_{MET} from both IVIVE models were input into a fish bioaccumulation model to estimate BCFs, which were then compared to literature BCF data. Estimated BCFs for all of the chemicals when considering biotransformation were lower than when biotransformation was assumed to be zero, indicating the importance in considering biotransformation when assessing bioaccumulation potential of chemicals. BCF estimates obtained from k_{MET} from both IVIVE models were in reasonable agreement with previous in-vitro biotransformation studies as well, indicating that in-vitro biotransformation assays are reproducible. However, further work is still needed to develop these in-vitro biotransformation assays to reflect the results from in-vivo biotransformation

studies, as evidenced by the substantial differences when comparing estimated BCFs from this study to empirical BCFs.

In-vitro biotransformation procedures allow for a quicker, more cost-effective method with reduced animal use when assessing the bioaccumulation potential of chemicals compared to traditional regulatory criteria which relies on K_{ow} values without the consideration of biotransformation. This study demonstrates the use of in-vitro substrate depletion experiments to assess the bioaccumulation potential of chemicals, and as further improvements to in vitro methods and IVIVE models occur, so should comparisons between in-vitro biotransformation studies and in vivo studies. Nevertheless, despite the current limitations, current in-vitro biotransformation methods of chemicals to assess bioaccumulation potential can still be useful as a screening tool prior to deciding if in-vivo studies are necessary or could be useful in a weight of evidence approach for bioaccumulation assessment as well. This can consequently allow for more informed and transparent screening of chemicals by regulatory agencies to ultimately protect the environment and humans.

5. References

Anzenbacher, P., Anzenbacherova, E. 2001. Cytochromes P450 and metabolism of xenobiotics. *Cellular and Molecular Life Sciences* 58 (5-6):737–747.

Arnot, J.A., and Gobas, F.A.P.C. 2004. A food web bioaccumulation model for organic chemicals in aquatic ecosystems. *Environmental Toxicology and Chemistry* 23:2343–2355.

Arnot, J.A. and Gobas, F.A.P.C. 2006. A review of bioconcentration factor (BCF) and bioaccumulation factor (BAF) assessments for organic chemicals in aquatic organisms. *Environmental Reviews* 14 (4): 257-297.

Arnot, J.A., Mackay, D., Bonnell, M. 2008. Estimating metabolic biotransformation rates in fish from laboratory data. *Enironmental Toxicology and Chemistry*.*27* (2): 345-351.

Austin, R. P., Barton, P., Cockroft, S. L., Wenlock, M. C., Riley, R. J. 2002. The influence of nonspecific microsomal binding on apparent intrinsic clearance, and its prediction from physicochemical properties. *Drug Metabolism and Disposition* 30(12): 1497-1503.

Berg J.M., Tymoczko,J.L., Stryer L. 2002. Biochemistry *5th Edition*. New York: W. H. Freeman and Company.

Bisswanger, H. 2008. Enzyme Kinetics: Principles and Methods. *2nd Edition*. Weinheim, Germany: Wiley-VCH.

Bradford, M.M. 1976. A rapid and sensitive method for the quantitation of microgram quantities of protein utilizing the principle of protein-dye binding. *Analytical Biochemistry* 72: 248-254.

Brandon, E.F.A., Raap, C.D., Meijerman I., Beijnen, J.H., Schellens J.H.M. 2003. An update on in vitro test methods in human hepatic drug biotransformation research: pros and cons. *Toxicology and Applied Pharmacology* 189:233–246.

Cederbaum, A.I. 2015. Molecular mechanisms of the microsomal mixed function oxidases and biological and pathological implications. *Redox Biology* 4:60-73.

Coecke, S., Ahr, H., Blaauboer, B., Bremer, S., Casati, S., Castell, J., Combes, R., Corvi, R., Crespi, C.L., Cunningham, M., Elaut, G., Eletti, B., Freidig, A., Gennari, A., Ghersi-Egea, J.F., Guillouzo, A., Hartung, T., Hoet, P., Ingelman-Sundberg, M., Worth, A. 2006. Metabolism: a bottleneck in in vitro toxicological test development. The Report and Recommendations of ECVAM Workshop 54. *Alternatives to Laboratory Animals* 34:49-84.

Cowan-Ellsberry, C. E., Dyer, S. D., Erhardt, S., Bernhard, M. J., Roe, A. L., Dowty, M. E., Weisbrod, A. V. 2008. Approach for extrapolating in vitro metabolism data to refine bioconcentration factor estimates. *Chemosphere* 70:1804–1817.

Crespi, C.L. 1995. Xenobiotic-metabolizing human cells as tools for pharmacological and toxicological research. *Advances in Drug Research* 26:179–235.

deBruyn, A.M., Gobas, F.A.P.C. 2007. The sorptive capacity of animal protein. *Environmental Toxicology and Chemistry* 26(9):1803-1808.

Di Giulio R.T. and Hinton D.E. 2008. The Toxicology of Fishes. United Kingdom: Taylor and Francis Group, CRC Press.

Dyer S.D., Bernhard M.J., Cowan-Ellsberry C., Perdu-Durand E., Demmerle S., Cravedi J-P. 2008. In vitro biotransformation of surfactants in fish. Part I: Linear alkylbenzene sulfonate (C12-LAS) and alcohol ethoxylate (C13EO8). *Chemosphere* 72 (5): 850-862.

Environment and Climate Change Canada. 2013. ARCHIVED - Guidance Manual for the Risk Evaluation Framework for Sections 199 and 200 of CEPA 1999: Decisions on Environmental Emergency Plans. Available online from https://www.ec.gc.ca/lcpe-cepa/default.asp?lang=En&n=F1BDDFD0-1&offset=3#s2_2 [Accessed on July 28,2017].

Escher, B. I., Cowan-Ellsberry, C. E., Dyer, S., Embry, M. R., Erhardt, S., Halder, M., Kwon, J. H., Johanning, K., Oosterwijk, M.T., Rutishauser, S., Segner, H., Nichols, J. 2011. Protein and lipid binding parameters in rainbow trout (*Oncorhynchus mykiss*) blood and liver fractions to extrapolate from an in vitro metabolic degradation assay to in vivo bioaccumulation potential of hydrophobic organic chemicals. *Chemical Research in Toxicology* 24(7): 1134-1143.

Fay, K. 2016. HESI Annual Meeting June 7, 2016 Presentation: In vitro to in vivo extrapolation of hepatic metabolism in fish: an inter-laboratory comparison of in vitro methods. Available online from http://hesiglobal.org/wp-content/uploads/sites/11/2016/06/Bioaccumulation-Committee-Presentation-2016.pdf [Accessed on November 7,2016].

Fay, K.A., Fitzsimmons, P.N., Hoffman, A.D., Nichols J.W. 2017. Comparison of trout hepatocytes and liver S9 fractions as in vitro models for predicting hepatic clearance in fish. *Environmental Toxicology and Chemistry* 36(2): 463-471.

Förlin, L., Lemaire, P., Livingstone, D. R. 1995. Comparative studies of hepatic xenobiotic metabolizing and antioxidant enzymes in different fish species. *Marine Environmental Research* 39 (1−4):201-204.

Franklin, C.E., Johnston, I.A., Crockford, T., Kamunde, C. 1995. Scaling of oxygen consumption of Lake Magadi tilapia, a fish living at 37^0C. *Journal of Fish Biology* 46:829-834.

Funari, E., Zoppini, A., Verdina, A., De Angelis, G., Vittozzi, L. 1987. Xenobiotic-metabolizing enzyme systems in test fish. *Ecotoxicology and Environmental Safety* 13: 24-31.

Gibson G.G. and Skett P. 1986. Introduction to Drug Metabolism. London, New York: Chapman and Hall.

Gomez, C. F., Constantine, L., Huggett, D. B. 2010. The influence of gill and liver metabolism on the predicted bioconcentration of three pharmaceuticals in fish. *Chemosphere* 81(10): 1189−1195.

Government of Canada. 1999. Canadian Environmental Protection Act, 1999. *Canada Gazette*, Part III, Vol 22; Public Works and Government Services: Ottawa, ON, 1999.

Gülden, M., Seibert, H. 2005. Impact of bioavailability on the correlation between in vitro cytotoxic and in vivo acute fish toxic concentrations of chemicals. *Aquatic Toxicology* 72(4): 327-337.

Guomao, Z., Yi, W., Jianying, H. 2016. Intrinsic clearance of xenobiotic chemicals by liver microsomes: assessment of trophic magnification potentials. *Environmental Science and Technology* 50: 6343-6353.

Han X., Nabb D.L., Mingoia R.T., Yang C.H. 2007. Determination of xenobiotic intrinsic clearance in freshly isolated hepatocytes from rainbow trout (*Oncorhynchus mykiss*) and rat and its application in bioaccumulation assessment. *Environmental Science and Technology* 41 (9): 3269-3276.

Han X., Nabb D.L., Yang C.H., Snajdr S.I., Hoke R. 2009. Liver microsomes and S9 from rainbow trout (*Oncorhynchus mykiss*): comparison of basal-level enzyme activities with rat and determination of xenobiotic intrinsic clearance in support of bioaccumulation assessment. *Environmental Toxicology and Chemistry* 28 (3): 481-488.

Hänninen, O., Lindström-Seppä, P., Pelkonen, K. Role of gut in xenobiotic metabolism. 1987. Archives of Toxicology 60(1−3), 34-36.

Hansen, D.J., Parrish, P.R. 1977. Suitability of sheepshead minnows (*Cyprinodon variegatus*) for life-cycle toxicity tests. In: F.L.Mayer and J.L.Hamelink (Eds.), *Aquatic Toxicology and Hazard Evaluation, 1st Symposium,* ASTM STP 634, Philadelphia, 3294 PA:117-126.

Heringa, M.B., Schreurs, R., Van der Saag, P.T., Van der Burg, B., Hermens, J.L.M. 2003. Measurement of free concentration as a more intrinsic dose parameter in an in vitro assay for estrogenic activity. *Chemical Research in Toxicology* 16: 1662-1663.

Johanning K., Hancock G., Escher B.I., Adelbayo B, Bernhardt M.J., Dyer S., Eickhoff C., Erhardt S., Johnson R., Halder M., Holden D., Rutishauser S., Segner H., Embry M., Fitzsimmons P., Nichols J. 2012a. Assessment of metabolic stability using rainbow trout (*Oncorhynchus mykiss*) liver S9 fractions. *Current Protocols in Toxicology* 53: 14.10.1-14.10.28.

Johanning, K., Hancock, G., Escher, B.I., Adekola, A., Bernhard, M., Cowan-Ellsberry, C., Domoradzki, J., Dyer, S., Eickhoff, C., Erhardt, S., Fitzsimmons, P., Halder, M., Nichols, J., Rutishauser, S., Sharpe, A., Segner, H., Schultz, I., Embry, M. 2012b. In vitro metabolism using rainbow trout liver S9 summary report of the HESI bioaccumulation committee. Available online from *http://www.hesiglobal.org/files/public/Committees/Bioaccumulation/Presentations%20and%20Data%20Resources/S9_report_FINAL_20Nov2012.pdf* [Accessed May 14, 2018].

Jonsson, G., Bechmann, R. K., Bamber, S. D., Baussant, T. 2004. Bioconcentration, biotransformation, and elimination of polycyclic aromatic hydrocarbons in sheepshead minnows (*Cyprinodon variegatus*) exposed to contaminated seawater. *Environmental Toxicology and Chemistry* 23:1538–1548.

Jordan, S.A., Feeley, M.M. 1999. PCB congener patterns in rats consuming diets containing Great Lakes salmon: analysis of fish, diets, and adipose tissue. *Environmental Research Section A* 80: S207-S212.

Kennedy, C., Gill, K., Walsh, P. 1991. *In-vitro* metabolism of benzo [a] pyrene in the blood of the Gulf toadfish, *Opsanus beta*. *Marine Environment Research* 31:37-53.

Kleinow, K.M., Melancon, M.J., Lech, J.J. 1987. Biotransformation and Induction: Implications for Toxicity, Bioaccumulation, and Monitoring of Environmental Xenobiotics in Fish. *Environmental Health Perspectives* 71: 105-119.

Kolanczyk, R.C., Fitzsimmons, P.N., McKim, J.M., Erickson, R.J., Schmieder, P.K. 2003. Effects of anesthesia (tricaine methanesulfonate, MS222) on liver biotransformation in rainbow trout (*Oncorhynchus mykiss*). *Aquatic Toxicology* 64:177–184.

Kwon, J.H., Wuethrich, T., Mayer, P., Escher, B.I. 2009. Development of a dynamic delivery method for in vitro bioassays. *Chemosphere* 76:83–90.

Laue H., Gfeller H., Jenner K.J., Nichols J.W., Kern S., Natsch A. 2014. Predicting the bioconcentration of fragrance ingredients by rainbow trout using measured rates of in vitro intrinsic clearance. *Environmental Science and Technology* 48: 9486-9495.

Lee, Y.S., Lee, D. H. Y., Delafoulhouze, M., Otton, S. V., Moore, M. M., Kennedy, C. J., Gobas, F. A. P. C. 2014. In vitro biotransformation rates in fish liver S9: effect of dosing techniques. *Environmental Toxicology and Chemistry* 33 (8):1885-1893.

Lee, Y.S., Lo, J.C., Otton, S.V., Moore, M.M., Kennedy, C.J., Gobas, F.A.P.C. 2017. In vitro to in vivo extrapolation of biotransformation rates for assessing bioaccumulation of hydrophobic organice chemicals in mammals. *Environmental Toxicology and Chemistry* 36 (7): 1934-1946.

Lo J.C., Allard G.N., Otton S.V., Campbell D.A., Gobas F.A.P.C. 2015a. Concentration dependence of biotransformation in fish liver S9: optimizing substrate concentrations to estimate hepatic clearance for bioaccumulation assessment. *Environmental Toxicology and Chemistry* 34: 2782-2790.

Lo, J.C., Campbell, D.A., Kennedy, C.J., Gobas, F.A.P.C. 2015b. Somatic and gastrointestinal in vivo biotransformation rates of hydrophobic chemicals in fish. *Environmental Toxicology and Chemistry* 34 (10): 2282-2294.

Lo, J.C., Letinski, D.J., Parkerton, T.F., Campbell, D.A., Gobas, F.A.P.C. 2016. In-vivo biotransformation rates of organic chemicals in fish: relationship with bioconcentration and biomagnification factors. *Environmental Science and Technology* 50:13299-13308.

Mingoia, R. T., Glover, K. P., Nabb, D. L., Yang, C.-H., Snajdr, S.I., Han, X. 2010. Cryopreserved hepatocytes from rainbow trout (*Oncorhynchus mykiss*): a validation study to support their application in bioaccumulation assessment. Environmental Science and Technology 44 (8):3052-3058.

Namdari, R. 1994. Pharmacokinetics of pyrene and oxytetracycline in salmonids. M.Sc. Thesis. Simon Fraser University, B.C. Canada.

Nath, A., Atkins, W.M. 2006. Short Communication: A Theoretical Validation of the Substrate Depletion Approach to Determining Kinetic Parameters. *Drug Metabolism and Disposition* 34 (9): 1433-1435.

Nabb, D. L., Mingoia, R. T., Yang, C. H., Han, X. 2006. Comparison of basal level metabolic enzyme activities of freshly isolated hepatocytes from rainbow trout (*Oncorhynchus mykiss*) and rat. *Aquatic Toxicology* 80(1): 52-59.

Nichols, J. W., Schultz, I. R., Fitzsimmons, P. N. 2006. In vitro–in vivo extrapolation of quantitative hepatic biotransformation data for fish. I. A review of methods, and strategies for incorporating intrinsic clearance estimates into chemical kinetic models. *Aquatic Toxicology* 78:74–90.

Nichols J., Erhardt S., Dyer S., James M., Moore M., Plotzke K., Segner H., Schultz. I., Thomas K., Vasiluk. L., Weisbrod A. 2007. Workshop report: use of *in vitro* absorption, distribution, metabolism, and excretion (ADME) data in bioaccumulation assessments for fish. *Human and Ecological Risk Assessment* 13 (6): 1164-1191.

Nichols, J.W., Bonnell, M., Dimitrov, S.D., Escher, B.I., Han, X., Kramer, N.I. 2009. Bioaccumulation assessment using predictive approaches. *Integrated Environmental Assessment and Management* 5(4):577-597.

Nichols, J.W., Huggett, D.B., Arnot, J.A., Fitzsimmons, P.N., Cowan-Ellsberry, C.E. 2013a. Towards improved models for predicting bioconcentration of well-metabolized compounds by rainbow trout using measured rates of in vitro intrinsic clearance. *Environmental Toxicology and Chemistry* 32 (7): 1611-1622.

Nichols, J. W., Hoffman, A. D., ter Laak, T. L., Fitzsimmons, P. N. 2013b. Hepatic clearance of 6 polycyclic aromatic hydrocarbons by isolated perfused trout livers: prediction from in vitro clearance by liver S9 fractions. *Toxicological Science* 136:359–372.

Mackay, D., Shiu, W.Y., Ma, K.C., Lee, S.C. 2006. Handbook of Physical-Chemical Properties and Environmental Fate for Organic Chemicals. Second Edition. CRC Press Vol. I-IV.

Obach, R. S. 1999. Prediction of human clearance of twenty-nine drugs from hepatic microsomal intrinsic clearance data: An examination of in vitro half-life approach and nonspecific binding to microsomes. *Drug Metabolism and Disposition* 27:1350–1359.

Obach, S.R., Reed-Hagen, A.E. 2002. Measurement of Michaelis constants for cytochrome P450-mediated biotransformation reactions using a substrate depletion approach. *Drug Metabolism and Disposition* 30 (7): 831-837.

OECD. 2012. OECD Guidelines for Testing Chemicals. Test No. 305: Bioaccumulation in Fish: Aqueous and Dietary Exposure; Organization for Economic Co-operation and Development: Paris.

OECD. 2017. Study report: multi-laboratory ring-trial to support development of OECD test guidelines on determination of in vitro intrinsic clearance using cryopreserved rainbow trout hepatocytes and liver S9 subcellular fractions. Available online from

https://www.oecd.org/env/ehs/testing/4OECD%20Draft%20ring%20trial%20study%20report%20for%20WNT.pdf [Accessed on May 29,2017].

Ogata, M., Fujisawa, K., Ogino, Y., Mano, E. 1984. Partition coefficients as a measure of bioconcentration potential of crude oil compounds in fish and shellfish. *The Bulletin of Environmental Contamination and Toxicology* 33:561-567.

Ohlberger, J., Mehner, T., Staaks, G., Holker, F. 2012. Intraspecific temperature dependence of the scaling of metabolic rate with body mass in fishes and its ecological implications. *Oikos* 121(2): 245-251.

Ramesh, A., Walker, S. A., Hood, D. B., Guillen, M. D., Schneider, K., Weyand, E. H. 2004. Bioavailability and risk assessment of orally ingested polycyclic aromatic hydrocarbons. *International Journal of Toxicology* 23:301-333.

Rane, A., Wilkinson, G. R., Shand, D. G. 1977. Prediction of hepatic extraction ratio from in vitro measurement of intrinsic clearance. *The Journal of Pharmacology and Experimental Therapeutics* 200:420-424.

Rogers, A., Gibson Y. 2009. '*Enzyme Kinetics: Theory & Practice'*. In: Plant Metabolic Networks (Schwender, J). Springer, New York. 71-103.

Schulz I.R., Hayton W.L. 1999. Interspecies scaling of the bioaccumulation of lipophilic xenobiotics in fish: An example using trifluralin. *Environmental Toxicology and Chemistry* 18 (7): 1440-1449.

Sohlenius-Sternbeck, A. K. 2006. Determination of the hepatocellularity number for human, dog, rabbit, rat and mouse livers from protein concentration measurements. *Toxicology in Vitro 20*:1582–1586.

Trowell, J.J., Gobas, F.A.P.C., Moore, M.M., Kennedy, C.J. 2018. Estimating the bioconcentration factors of hydrophobic organic compounds from biotransformation rates using rainbow trout hepatocytes. *Archives of Environmental Contamination and Toxicology* 75 (2): 295-305.

UNEP (United Nations Environment Programme). 2013. Global Chemicals Outlook: Towards Sound Management of Chemicals. Available online from https://wedocs.unep.org/bitstream/handle/20.500.11822/8455/Global%20chemicals%20outlook_%20towards%20sound%20management%20of%20chemicals2013Global%20Chemicals%20Outlook.pdf?amp%3BisAllowed=&sequence=3 [Accessed on July 20, 2017].

Uno, T., Ishizuka, M., Itakura, T. 2012. Cytochrome P450 (CYP) in fish. *Environmental Toxicology and Pharmacology* 34: 1-13.

Weisbrod A. V., Sahi J. Segner H., James M.O., Nichols J., Schultz I., Erhardt S., Cowan-Ellsberry C., Bonnell M., Hoeger B. 2009. The state of in-vitro science for use in bioaccumulation assessments for fish. *Environmental Toxicology and Chemistry* 28 (1): 86-96.

Wilkinson, G.R., Shand, D.G. 1975. Commentary: a physiological approach to hepatic drug clearance. *Clinical Pharmacology and Therapeutics* 18 (4): 377-390.

APPENDICES

Appendix A. GC/MS Standard Curves

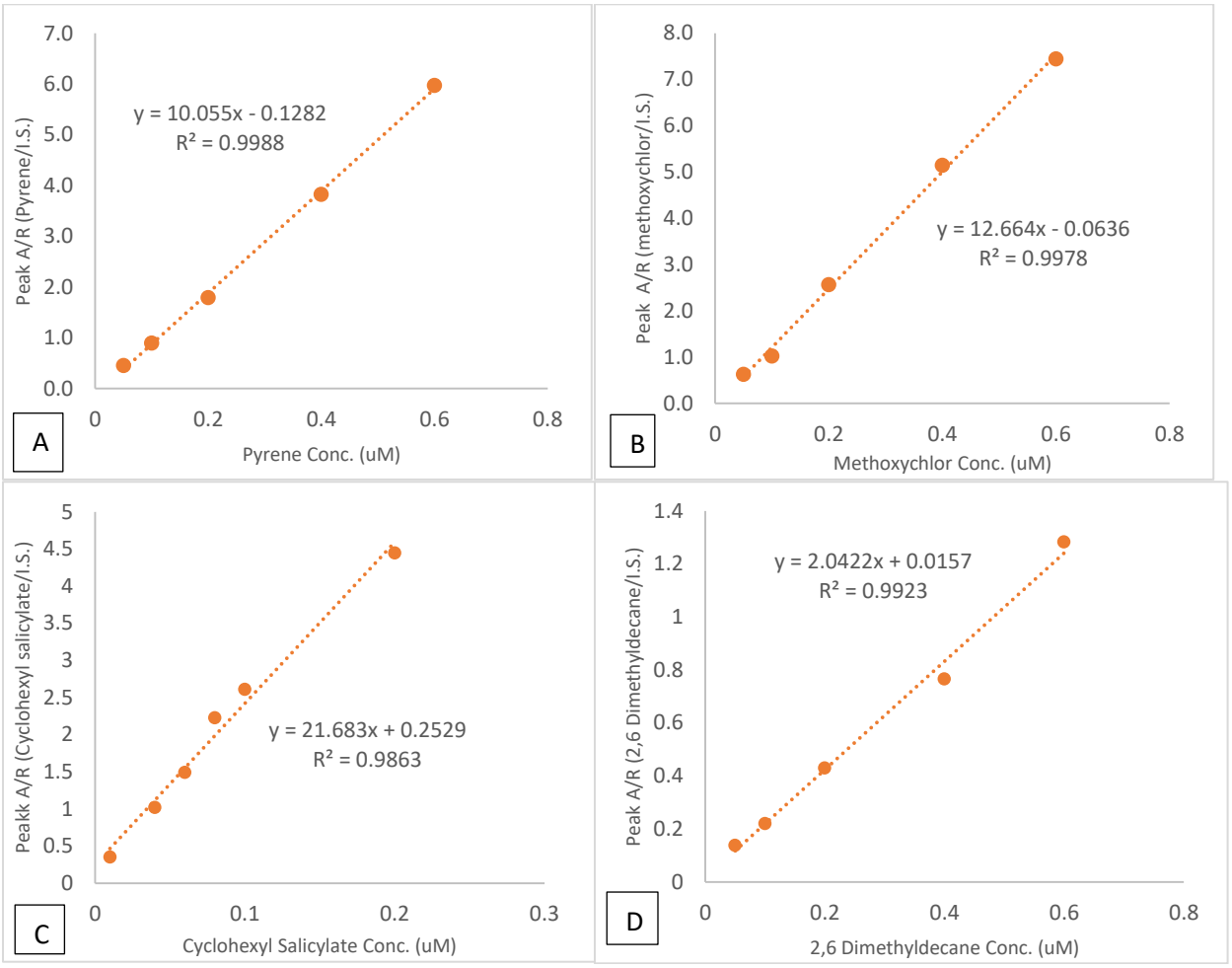

Figure A-1. Standard curves for pyrene (A), methoxychlor (B), cyclohexyl salicylate (C), and 2,6 dimethyldecane illustrating response, measured as the peak area of test chemical to chrysene d-12 internal standard (I.S.) as a function of chemical concentration.

Appendix B. Protein content of Liver S9 fractions

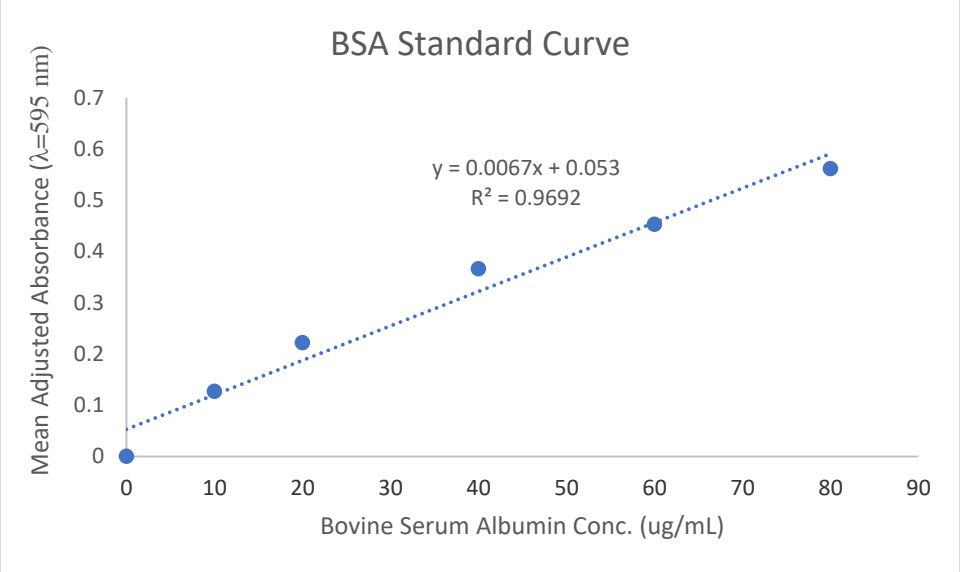

Figure B-2. Blank corrected bovine serum albumin (BSA) calibration curve showing the mean absorbance (n=3) at various BSA concentrations.

Table B-1. Dilution calculations for standard curve stock solutions. Initial concentration of Bovine Serum Albumin (BSA) stock solution was 2 mg/mL.

[BSA second stock] (µg/mL)	0	10	20	40	60	80
Volume BSA (µL) pipetted out from the first stock 2 mg/mL	0	5	10	20	30	40
Volume Buffer (µL)	1000	995	990	980	970	960
Amount of Protein (ug protein/well)	0	0.5	1.0	2.0	3.0	4.0

Table B-2. Dilution calculations to create S9 dilution samples.

[S9] (mg/mL)	0.04	0.06	0.07	0.08
Volume (µL) pipetted out from the unknowns whose concentrations are supposed to be 20-30 mg/mL	2	3	3.5	4
Volume buffer (µL)	1248	1247	1246.5	1246

Table B-3. Blank corrected mean absorbance (n=3) of BSA standards (λ=595 nm).

BSA Standard (mg/mL)	Mean Absorbance	Mean Adjusted Absorbance
0	0.455	0
0.01	0.582	0.127
0.02	0.677	0.222
0.04	0.821	0.366
0.06	0.908	0.453
0.08	1.017	0.562

Table B-4. Blank corrected mean absorbance (n=3) (λ=595 nm) of S9 diluted samples. S9 dilution concentrations were selected assuming that S9 has a protein content between 20-30 mg/mL when diluted 1:1 in buffer, and diluted to a concentration between 0.5 to 4 µg in 50 µL (assay volume). S9 dilution samples were made in 1250 uL autosampler vials prior to assaying. All concentrations are mg/mL.

Concentration of s9 dilution samples (mg/mL)	Mean Blank Adjusted Absorbance	Mean [protein] corresponding to standard curve	[S9] adjusted for volume	[S9] adjusted for amount added	Concentration of S9 samples
0.04	0.347	43.88	54.85	27.43	27.43
0.06	0.444	58.36	72.95	24.32	24.32
0.07	0.485	64.48	80.60	23.03	23.03
0.08	0.547	73.73	92.16	23.04	23.04

Appendix C: Extraction Efficiency Tests

Table C-1. Pyrene (Pyr) extraction efficiency of standards made in hexane. The retention time (RT), peak area (Pk A), and the peak area ratio of test chemical to internal standard (d-12 chrysene) is displayed. The average and standard deviation (SD) are displayed as well.

STANDARD REP.	**RT (Pyr)**	**RT (d-12)**	**Pk A (Pyr)**	**Pk A (d-12)**	**Pk A/R (Pyr/d-12)**
1	10.513	11.917	1471	2412	0.610
2	10.517	11.917	1395	2373	0.588
3	10.517	11.917	1874	1873	1.001
AVG.			1580.0	2219.3	0.733
SD			257.4	300.6	0.232

Table C-2. Pyrene extraction efficiency of pyrene samples. The retention time (RT), peak area (Pk A), and the peak area ratio of test chemical to internal standard (d-12 chrysene) is displayed. The average and standard deviation (SD) are displayed as well.

EE REP.	**RT (Pyr)**	**RT (d-12)**	**Pk A (Pyr)**	**Pk A (d-12)**	**Pk A/R (Pyr/d-12)**
1	10.513	11.917	1802	2532	0.712
2	10.517	11.921	1518	1667	0.911
3	10.513	11.913	1627	2172	0.749
AVG.			1649.0	2123.7	0.790

SD			143.3	434.5	0.106

Table C-3. Methoxychlor (MC) extraction efficiency of standards made in hexane. The retention time (RT), peak area (Pk A), and the peak area ratio of test chemical to internal standard (d-12 chrysene) is displayed. The average and standard deviation (SD) are displayed as well.

STANDARD REP.	RT (MC)	RT (d-12)	Pk A (MC)	Pk A (d-12)	Pk A/R (MC/d-12)
1	12.581	12.726	2801	1693	1.654
2	12.581	12.726	3220	1868	1.724
3	12.581	12.581	3667	2164	1.695
AVG.			3229.3	1908.3	1.691
SD			433.1	238.1	0.035

Table C-4. Methoxychlor (MC) extraction efficiency results from extraction samples. The retention time (RT), peak area (Pk A), and the peak area ratio of test chemical to internal standard (d-12 chrysene) is displayed. The average and standard deviation (SD) are displayed.

EE Rep.	RT (MC)	RT (d-12)	Pk A (MC)	Pk A (d-12)	Pk A/R (MC/d-12)
1	12.581	12.72	3131	2017	1.552
2	12.575	12.72	3904	2152	1.814
3	12.581	12.72	3365	1876	1.794
AVG.			3466.7	2015.0	1.720
SD			396.4	138.0	0.146

Table C-5. Cyclohexyl salicylate (CS) extraction efficiency of standards made in hexane. The retention time (RT), peak area (Pk A), and the peak area ratio of test chemical to internal standard (d-12 chrysene) is displayed. The average and standard deviation (SD) are displayed.

STANDARD REP.	RT (CS)	RT (d-12)	Pk A (CS)	Pk A (d-12)	Pk A/R (CS/d-12)
1	8.988	12.104	813	1166	0.697
2	8.988	12.104	896	1315	0.681
3	8.988	12.104	677	1246	0.543
AVG.			795.33	1242.33	0.641
SD.			110.56	74.57	0.085

Table C-6. Cyclohexyl salicylate (CS) extraction efficiency results from extraction samples. The retention time (RT), peak area (Pk A), and the peak area ratio of test chemical to internal standard (d-12 chrysene) is displayed. The average and standard deviation (SD) are displayed.

EE Rep.	RT (CS)	RT (d-12)	Pk A (CS)	Pk A (d-12)	Pk A/R (CS/d-12)
1	8.988	12.1	1415	1678	0.84
2	8.984	12.1	1201	1350	0.89
3	8.988	12.096	1284	1858	0.69
AVG.			1300.00	1628.67	0.81
SD			107.89	257.57	0.10

Table C-7. 2,6 dimethyldecane (2,6 DMD) extraction efficiency of standards made in hexane. The retention time (RT), peak area (Pk A), and the peak area ratio of test chemical to internal standard (d-12 chrysene) is displayed. The average and standard deviation (SD) are displayed.

STANDARD REP.	RT (2,6 DMD)	RT (d-12)	Pk A (2,6 DMD)	Pk A (d-12)	Pk A/R (2,6 DMD/d-12)
1	6.402	13.697	175056	766574	0.228
2	6.402	13.681	156756	745839	0.210
3	6.394	13.681	149223	760755	0.196
AVG.			160345	757723	0.212
SD			13285	10695	0.016

Table C-8. 2,6 dimethyldecane (2,6 DMD) extraction efficiency results from extraction samples. The retention time (RT), peak area (Pk A), and the peak area ratio of test chemical to internal standard (d-12 chrysene) is displayed. The average and standard deviation (SD) are displayed.

EE Rep.	RT (2,6 DMD)	RT (d-12)	Pk A (2,6 DMD)	Pk A (d-12)	Pk A/R (2,6 DMD/d-12)
1	6.394	13.674	83390	662139	0.126
2	6.394	13.681	61774	805520	0.077
3	6.394	13.658	67438	617438	0.109
AVG.			70867.33	695032.33	0.10
SD			11208.62	98260.82	0.03

Appendix D: Substrate Depletion Data

Table D-1. Pyrene depletion data from pyrene incubations with methoxychlor. The substrate concentration (μM) in the active and inactive S9 is displayed, along with the natural logarithm of the concentration in the active S9 over the concentration in the inactive S9. The slope, intercept and R^2 are displayed as well. / are data that was omitted from k_{dep} determination due to the possibility of enzyme attenuation.

Replicate 1. Pyrene with methoxychlor				
Time (min.)	**Active S9**	**Inactive S9**	**Active/Inactive**	**Ln Active/Inactive**
0	0.077	0.160	0.480	-0.734
15	0.048	0.175	0.273	-1.299
30	0.034	0.174	0.193	-1.643
45	0.026	0.173	0.152	-1.886
60	0.018	0.172	0.104	-2.262
75	0.015	0.171	0.091	-2.401
90	0.012	0.170	0.071	-2.649
slope				-0.204
intercept				-0.921
R2				0.97
Replicate 2. Pyrene with methoxychlor				
Time (min.)	**Active S9**	**Inactive S9**	**Active/Inactive**	**Ln Active/Inactive**

0	0.074	0.160	0.463	-0.771
15	0.055	0.175	0.313	-1.162
30	0.042	0.174	0.240	-1.427
45	0.029	0.173	0.169	-1.777
60	0.026	0.172	0.152	-1.884
75	0.021	0.171	0.125	-2.079
90	0.015	0.170	0.089	-2.416
slope				-0.172
intercept				-0.871
R2				0.98
Replicate 3. Pyrene with methoxychlor				
Time (min.)	**Active S9**	**Inactive S9**	**Active/Inactive**	**Ln Active/Inactive**
0	0.084	0.160	0.523	-0.648
15	0.059	0.175	0.338	-1.084
30	0.039	0.174	0.225	-1.493
45	0.034	0.173	0.194	-1.639
60	0.016	0.172	0.094	-2.363
75	0.018	0.171	0.103	-2.275
90	0.013	0.170	0.074	-2.604
slope				-0.022
intercept				-0.753
R2				0.95

Table D-2. Pyrene depletion data from pyrene incubations with cyclohexyl salicylate. The substrate concentration (μM) in the active and inactive S9 is displayed, along with the natural logarithm of the concentration in the active S9 over the concentration in the inactive S9. The slope, intercept and R^2 are displayed as well. / are data that was omitted from k_{dep} determination due to the possibility of enzyme attenuation.

Replicate 1. Pyrene with cyclohexyl salicylate				
Time (min.)	**Active S9**	**Inactive S9**	**Active S9/Inactive S9**	**Ln Active S9/Inactive S9**
0	0.182	0.160	1.140	0.131
5	0.187	0.176	1.062	0.060
10	0.169	0.187	0.906	-0.098
15	0.154	0.175	0.877	-0.131
20	0.131	0.183	0.714	-0.338
25	0.089	0.175	0.507	-0.679
slope				-0.301
intercept				0.201
R2				0.91
Replicate 2. Pyrene with cyclohexyl salicylate				
Time (min.)	**Active S9**	**Inactive S9**	**Active S9/Inactive S9**	**Ln Active S9/Inactive S9**
0	0.181	0.160	1.132	0.124

5	0.180	0.176	1.021	0.021
10	0.122	0.187	0.655	-0.423
15	0.122	0.175	0.694	-0.365
20	0.113	0.183	0.619	-0.480
25	/	/	/	/
slope				-0.319
intercept				0.094
R2				0.83
Replicate 3. Pyrene with cyclohexyl salicylate				
Time (min.)	**Active S9**	**Inactive S9**	**Active S9/Inactive S9**	**Ln Active S9/Inactive S9**
0	0.170	0.160	1.063	0.061
5	0.195	0.176	1.107	0.101
10	0.175	0.187	0.934	-0.068
15	0.168	0.175	0.958	-0.043
20	0.150	0.183	0.818	-0.201
25	0.091	0.175	0.521	-0.652
slope				-0.254
intercept				0.184
R2				0.75

Table D-3. Pyrene depletion data from pyrene incubations 2,6 dimethyldecane. The substrate concentration (μM) in the active and inactive S9 is displayed, along with the natural logarithm of the concentration in the active S9 over the concentration in the inactive S9. The slope, intercept and R^2 are displayed as well. / are data that was omitted from k_{dep} determination due to the possibility of enzyme attenuation.

Replicate 1. Pyrene with 2,6 dimethyldecane				
Time (min.)	**Active S9**	**Inactive S9**	**Active S9/Inactive S9**	**Ln Active S9/Inactive S9**
0	0.275	0.160	1.720	0.542
17.5	0.159	0.175	0.908	-0.097
35	0.199	0.174	1.146	0.136
52.5	0.114	0.173	0.661	-0.414
70	0.113	0.171	0.662	-0.413
87.5	0.086	0.170	0.506	-0.682
slope				-0.124
intercept				0.39
R2				0.84
Replicate 2. Pyrene with 2,6 dimethyldecane				
Time (min.)	**Active S9**	**Inactive S9**	**Active S9/Inactive S9**	**Ln Active S9/Inactive S9**
0	0.152	0.160	0.950	-0.051

10	0.130	0.187	0.694	-0.366
20	0.107	0.183	0.585	-0.536
30	0.122	0.181	0.678	-0.388
40	0.103	0.173	0.595	-0.518
50	0.090	0.164	0.549	-0.600
slope				-0.009
intercept				-0.1914
R2				0.68
Replicate 3. Pyrene with 2,6 dimethyldecane				
Time (min.)	**Active S9**	**Inactive S9**	**Active S9/Inactive S9**	**Ln Active S9/Inactive S9**
0	0.163	0.160	1.018	0.018
10	0.130	0.187	0.696	-0.362
20	0.111	0.183	0.605	-0.502
30	0.116	0.181	0.642	-0.443
40	0.096	0.173	0.558	-0.583
50	0.079	0.164	0.478	-0.737
slope				-0.125
intercept				-0.122
R2				0.84

Table D-4. Methoxychlor depletion data. The substrate concentration (μM) in the active and inactive S9 is displayed, along with the natural logarithm of the concentration in the active S9 over the concentration in the inactive S9. The slope, intercept and R^2 are displayed as well. / are data that was omitted from k_{dep} determination due to the possibility of enzyme attenuation.

Methoxychlor Replicate 1				
Time (min.)	**Active S9**	**Inactive S9**	**Active S9/Inactive S9**	**Ln Active S9/Inactive S9**
0	0.074	0.090	0.819	-0.200
15	0.067	0.092	0.726	-0.320
30	0.060	0.092	0.657	-0.421
45	0.054	0.089	0.608	-0.497
60	0.042	0.169	0.251	-1.383
75	0.034	0.163	0.210	-1.560
90	0.050	0.165	0.302	-1.196
slope				-0.015
intercept				-0.108
R2				0.78
Methoxychlor Replicate 2				
Time (min.)	**Active S9**	**Inactive S9**	**Active S9/Inactive S9**	**Ln Active S9/Inactive S9**
0	0.068	0.097	0.696	-0.363

15	0.064	0.103	0.624	-0.472
30	0.074	0.099	0.744	-0.296
45	0.048	0.100	0.476	-0.743
60	0.061	0.178	0.342	-1.073
75	0.033	0.180	0.185	-1.687
90	0.028	0.174	0.163	-1.812
slope				-0.018
intercept				-0.113
R2				0.87
Methoxychlor Replicate 3				
Time (min.)	**Active S9**	**Inactive S9**	**Active S9/Inactive S9**	**Ln Active S9/Inactive S9**
0	0.067	0.094	0.717	-0.333
15	0.081	0.103	0.787	-0.239
30	0.038	0.097	0.389	-0.945
45	0.036	0.092	0.391	-0.939
60	0.026	0.183	0.140	-1.964
75	0.029	0.184	0.155	-1.865
90	0.023	0.106	0.221	-1.512
slope				-0.019
intercept				-0.278
R2				0.76

Table D-5. Cyclohexyl salicylate depletion data. The substrate concentration (μM) in the active and inactive S9 is displayed, along with the natural logarithm of the concentration in the active S9 over the concentration in the inactive S9. The slope, intercept and R^2 are displayed as well. / are data that was omitted from k_{dep} determination due to the possibility of enzyme attenuation.

Cyclohexyl Salicylate Replicate 1				
Time (min.)	**Active S9**	**Inactive S9**	**Active S9/Inactive S9**	**Ln Active S9/Inactive S9**
0	0.118	0.504	0.234	-1.450
5	0.130	0.485	0.269	-1.314
10	0.052	0.480	0.108	-2.228
15	0.021	0.577	0.036	-3.331
20	0.007	0.543	0.012	-4.398
25	0.004	0.483	0.009	-4.732
slope				-0.153
intercept				-0.998
R2				0.94
Cyclohexyl Salicylate Replicate 2				
Time (min.)	**Active S9**	**Inactive S9**	**Active S9/Inactive S9**	**Ln Active S9/Inactive S9**
0	0.853	0.549	1.553	0.440
5	0.097	0.471	0.206	-1.582

10	0.020	0.590	0.034	-3.394
15	0.003	0.543	0.005	-5.367
20	0.001	0.505	0.003	-5.889
25	/	/	/	/
slope				-0.329
intercept				0.13
R2				0.97
Cyclohexyl Salicylate Replicate 3				
Time (min.)	**Active S9**	**Inactive S9**	**Active S9/Inactive S9**	**Ln Active S9/Inactive S9**
0	0.252	0.541	0.466	-0.763
5	0.156	0.546	0.286	-1.252
10	0.084	0.558	0.150	-1.897
15	0.021	0.480	0.044	-3.125
20	0.014	0.517	0.027	-3.619
25	0.012	0.471	0.026	-3.635
slope				-0.13
intercept				-0.761
R2				0.94

Table D-6. 2,6 dimethyldecane depletion data. The substrate concentration (μM) in the active and inactive S9 is displayed, along with the natural logarithm of the concentration in the active S9 over the concentration in the inactive S9. The slope, intercept and R^2 are displayed as well. / are data that was omitted from k_{dep} determination due to the possibility of enzyme attenuation.

2,6 dimethyldecane Replicate 1				
Time (min.)	**Active S9**	**Inactive S9**	**Active S9/Inactive S9**	**Ln Active S9/Inactive S9**
0	0.134	0.158	0.849	-0.164
17.5	/	/	/	/
35	0.041	0.161	0.253	-1.374
52.5	0.065	0.153	0.427	-0.851
70	0.066	0.149	0.440	-0.820
87.5	0.069	0.151	0.456	-0.785
slope				0.005
intercept				-0.549
R2				0.16
2,6 dimethyldecane Replicate 2				
Time (min.)	**Active S9**	**Inactive S9**	**Active S9/Inactive S9**	**Ln Active S9/Inactive S9**
0	0.220	0.154	1.425	0.354
10	0.204	0.157	1.298	0.261

20	0.350	0.261	1.341	0.293
30	0.289	0.289	0.999	-0.001
40	0.236	0.240	0.986	-0.015
50	/	/	/	/
slope				-0.01
intercept				0.379
R2				0.83
2,6 dimethyldecane Replicate 3				
Time (min.)	**Active S9**	**Inactive S9**	**Active S9/Inactive S9**	**Ln Active S9/Inactive S9**
0	0.242	0.248	0.977	-0.023
10	0.287	0.243	1.184	0.169
20	0.282	0.267	1.054	0.053
30	/	/	/	/
40	0.216	0.314	0.687	-0.376
50	/	/	/	/
slope				-0.01
intercept				0.1396
R2				0.58

Appendix E: IVIVE and fish bioaccumulation model parameters

Table E-1. IVIVE parameters for the Nichols et al. (2013a) model.

PARAMETER	VALUE	UNITS	REFERENCE
K_{OW}		Unitless	-
Log K_{OW}		Unitless	-
Body weight of fish used for S9 (B_{wgS9})	1500	g	-
S9 protein concentration (C_{S9})	1	mg/mL	-
Reaction Rate (*Rate*)		1/h	-
Fish Holding Temperature (*T*)	15	Celsius	-
Liver S9 protein content (L_{s9})	163	mg/g liver	Nichols et al. 2013
Liver weight as fraction of whole body weight (L_{FBW})	0.015	Unitless	Schultz and Hayton 1999
Liver blood flow as fraction of cardiac output (Q_{HFRAC})	0.259	Unitless	Nichols et al. 1990
Fractional water content of blood (v_{WBL})	0.84	Unitless	Bertelson et al. 1998

Fractional whole body lipid content (v_{LWB})	0.05	Unitless	Nichols et al. 2013a
Body Weight of modelled fish (Bw_{kgM})	0.01	kg	-
In vitro intrinsic clearance ($CL_{in\ vitro,\ int}$)	Rate/C_{S9}	ml/h/mg protein	Nichols et al. 2013a
In vivo intrinsic clearance ($CL_{in\ vivo,\ int}$)	$CL_{IN\ VITRO,INT} * L_{S9} * L_{FBW} * 24$	L/d/kg	Nichols et al. 2013a
Unbound fraction in the S9 system ($f_{U,S9}$)	$1/(C_{S9}{}^{*100.694\ log\ Kow-2.158}+1.0)$	Unitless	Han et al. 2009
Blood to water partition coefficient (P_{BW})	$(10^{0.73*log\ KOW} * 0.16) + 0.84$	Unitless	Fitzsimmons et al. 2001
Unbound fraction in blood plasma ($f_{U,P}$)	v_{WBL}/P_{BW}	Unitless	Nichols et al. 2013a
Hepatic clearance binding term (f_U)	$f_{u,p}/f_{u,S9}$	Unitless	Nichols et al. 2013a
Cardiac output, scaled to temp. and body weight (Q_C)	$[(0.23*T)-0.78]*(Bwg_m/500)^{-0.1} * 24$	L/d/kg fish	Erickson and McKim 1990
Blood flow to the liver (Q_H)	Q_C*Q_{HFRAC}	L/d/kg fish	Nichols et al. 2013a
Hepatic clearance (CL_H)	$((Q_H*f_U*CL_{IN\ VIVO,INT,10})/(Q_H+(f_U*CL_{IN\ VIVO,INT,10}))$	L/d/kg liver	Wilkinson and Shand 1975
Partitioning-based BCF (BCF_P)	$v_{LWB}*K_{OW}$	Unitless	Arnot and Gobas 2004
Apparent volume of distribution ($V_{D,BL}$)	BCF_P/P_{BW}	L/kg	Nichols et al. 2013a
Whole-body metabolism rate constant (k_{MET})	$CL_H/V_{D,BL}$	1/d	Nichols et al. 2013a

Table E-2. Parameters for fish bioaccumulation model (Arnot and Gobas 2003).

PARAMETER	VALUE	UNITS	REFERENCE
Particulate organic carbon content (C_{POC})	$5.0 * 10^{-7}$	kg/L	Arnot and Gobas 2003
POC binding constant (α_{POC})	0.35	Unitless	Seth et al. 1999
Dissolved organic carbon content (C_{DOC})	$5.0 * 10^{-7}$	kg/L	Arnot and Gobas 2003
DOC affinity constant (α_{DOC})	0.08	Unitless	Burkhard 2000
Total aqueous chemical concentration ($C_{W,TOT}$)	1	mg/L	-
Gill uptake rate constant (k_1)	$1/ [(0.01 + 1/K_{OW}) * B_{wkgM}{}^{0.4}]$	L/d/kg fish	Arnot and Gobas 2003
Gill elimination rate constant (k_2)	k_1/BCF_P	1/d	Arnot and Gobas 2003
Fecal egestion rate constant (k_E)	$0.125[0.02\ B_{wkgM}{}^{-0.15}e^{(0.06*1)}/ (5.1 \times 10^{-8}*K_{OW} + 2)]$	1/d	Arnot and Gobas 2003
Freely dissolved chemical fraction in water (FD)	$1/(1+C_{POC}*\alpha_{POC}*K_{OW}+C_{DOC}*\alpha_{DOC}*K_{OW})$	Unitless	Arnot and Gobas 2003
Freely dissolved chemical concentration in water ($C_{W,FD}$)	$C_{W,TOT} * FD$	mg/L	Arnot and Gobas 2003

Steady-state chemical concentration in fish ($C_{FISH,SS}$)	$k_1 * C_{W,FD}/ (k_2+k_{MET}+k_E)$	mg/kg	Arnot and Gobas 2003
BCF expressed on a total chemical basis (BCF_{TOT})	$C_{FISH,SS}/C_{W,TOT}$	L/kg	Arnot and Gobas 2003

Table E-3. IVIVE parameters for the Lee et al. (2017) model.

PARAMETER	VALUE	UNITS	REFERENCE
In vitro biotransformation rate constant ($k_{dep,C\rightarrow0}$)		hr^{-1}	-
Fraction unbound of chemical ($f_{u,inc.}$)	$\log\left(\frac{1-f_{u,inc}}{f_{u,inc}}\right) = 0.73*\log K_{OW} + 0.83 *\log C_{S9} + (-2.30)$	Unitless	Lo 2018
Maximum in vitro biotransformation rate constant ($\mathbf{k^*_{dep,C\rightarrow0}}$)	$k_{dep,C\rightarrow0})/ f_{u,inc}$.	hr^{-1}	Lee et al. 2017
Volume of incubation ($V_{inc.}$)		mL	-
Volume of S9 for incubation ($V_{S9,inc.}$)		mL	-
Volume of liver S9 fraction collected after centrifugation (V_{S9})	28.9	mL	Lee et al. 2017 Obtained from Lo 2018
Wet weight of liver (W_H)	23.4	g	-
Density of liver (D_H)	1.05	g/mL	Sohlenius-Sternbeck 2006
Fraction of water in the liver ($f_{W,H}$)	0.73	Unitless	Lo 2018
Fraction of lipid in the liver ($f_{L,H}$)	0.06	Unitless	Lo 2018
Fraction of protein in the liver ($f_{P,H}$)	0.21	Unitless	Lo 2018
Sorptive capacity of proteins relative to that of lipids for animal protein (*X*)	0.05	Unitless	deBruyne and Gobas 2007
Kow		Unitless	-
Volume of liver (V_H)	22.3	mL	-
Volume of organism (V_B)	1500	mL	-
Mass of liver ($mass_H$)	23.4	g	-
Mass of fish ($mass_B$)	1.5	kg	-
Density of fish ($density_B$)	1000	kg/m^3	Lee et al. 2017
Fraction of lipid in organism ($f_{L,B}$)	0.06	Unitless	Lo 2018
Fraction of protein in organism ($f_{P,B}$)	0.19	Unitless	Lo 2018
Fraction of water in	0.75	Unitless	Lo 2018

organism ($f_{W,B}$)			

Appendix F: Empirical BCF data

Table F-1. Compiled BCF values derived through *in-vivo* studies from the literature.

Chemical	BCF Value	Test Species	Reference
Pyrene	484	Goldfish (*Carassius auratus*)	Ogata et al. 1984
	97-145	Sheepheads minnow (*Cyorinodon variegates*)	Jonsson et al. 2004
Methoxychlor	174	Sheepheads minnow (*Cyorinodon variegates*)	Hansen and Parrish 1977
Cyclohexyl salicylate	440	Rainbow trout (*Oncorhynchus mykiss*)	Chen et al. 2018
	600-900	Zebrafish (*Danio rerio*)	Laue et al. 2014 RIFM study *Obtained from ECHA dossier
2,6 dimethyldecane	910	Rainbow trout (*Oncorhynchus mykiss*)	Lo et al. 2016